JOURNAL OF GEOPHYSICAL RESEARCH, VOL. 104, NO. B10, PAGES 23,033–23,049, OCTOBER 10, 1999

Thermal and mechanical aspects of magma emplacement in giant dike swarms

Yuri A. Fialko[1] and Allan M. Rubin

Department of Geosciences, Princeton University, Princeton, New Jersey

Abstract. We consider the thermal history and dynamics of magma emplacement in giant feeder dikes associated with continental flood basalts. For driving pressure gradients inferred for giant dike swarms, thicknesses of <10 m would enable dikes to transport magma laterally over the distances observed in the field (up to thousands of kilometers) without suffering thermal lock-up. Using time-dependent numerical solutions for the thermal evolution of a dike channel under laminar and turbulent flow conditions in the presence of phase transitions, we investigate the possibility that the observed dike thicknesses (of the order of 100 m) result from thermal erosion of the country rocks during dike emplacement. This implies that the observed range of dike widths in giant dike swarms may reflect variations in the source volume and not the excess magma pressure. It is found that the total volume of intruded magma required to produce an order of magnitude increase in dike width via wall rock melting broadly agrees with the estimated volumes of individual flows in continental flood basalts. The presence of chilled margins and apparently low crustal contamination characteristics of some giant dikes may be consistent with turbulent magma flow and extensive melt back during dike emplacement. In this case, measurements of the anisotropy of magnetic susceptibility most likely indicate magma flow directions during the final stages of dike intrusion. Shear stresses generated at the dike wall when the dike starts to freeze strongly decrease with increasing dike width, which implies that thicker dikes may have less tendency to produce consistent fabric alignment. Our results suggest that if the dike was propagating downslope off a plume-related topographic swell, the mechanism responsible for flow termination could possibly have been related to underpressurization and collapse (implosion) of the shallow magma plumbing system feeding the intrusion. Radial dikes that erupted at the periphery of the topographic uplift might have increased (rather than decreased) extensional stresses in the crust within the topographic uplift upon their solidification.

1. Introduction

Giant dike swarms represent spectacular traces of magmatic events that are characterized by perhaps the highest magma production and effusion rates in the geologic record (a comprehensive review of giant dike swarms is given by *Ernst et al.* [1995]; see also *Halls and Fahrig* [1987] and *Parker et al.* [1990]). The term "giant" reflects that the scale of these dike swarms is unparalleled in currently active basaltic systems. Individual dikes in giant swarms range in thickness from tens to hundreds of meters and extend laterally for distances of several hundreds to a few thousands of kilometers [*Fahrig*, 1987]. This may be compared with dike widths of a few meters and maximum propagation distances of the order of 10^2 km typical of volcanic centers in Iceland, Hawaii and on the mid-ocean ridges [*Einarsson and Brandsdottir*, 1980; *Klein et al.*, 1987; *Fox et al.*, 1995]. While the origin of giant dike swarms is still uncertain, it is likely that production of large volumes of melt in relatively short periods of time (typically ~10^6 years or less for the whole magmatic event [*White and McKenzie*, 1989; *Coffin and Eldholm*, 1994]) requires a major thermal perturbation in the upper mantle. High magma fluxes associated with giant dike swarms and flood basalts (for which giant dikes are believed to be the feeder conduits) have led to the suggestion of mantle plumes as a possible source [e.g., *LeCheminant and Heaman*, 1989]. In this case, flood volcanism is thought to manifest arrivals of giant plume heads that spread at the base of the lithosphere and release large volumes of magma by decompressional melting [*Griffiths and Campbell*, 1990; *Duncan and Richards*, 1991]. Indeed, many flood basalt provinces seem to initiate hotspot tracks that presumably mark the subsequent motion of the lithosphere over the plume "stems" [*Morgan*, 1971, 1983]. Additional evidence for mantle plume involvement includes topographic doming associated with magma emplacement [*Cox*, 1989] and peculiar geochemical signatures of flood basalts [e.g., *Lassiter and DePaolo*, 1997]. Alternative (to mantle plume) hypotheses of the origin of flood volcanism advocate shallow (i.e., upper mantle) magma sources and emphasize the importance of lithospheric controls on the occurrence of flood volcanism [e.g., *Anderson*, 1998].

Giant dike swarms associated with continental flood basalts commonly exhibit a radiating or fanning pattern focused on the center of the inferred topographic uplift [*Ernst and Buchan*, 1997] and extend up to 2000 km from the magmatic center. Similar radial fracture systems consisting of a large number of lineations extending up to 2000 km from inferred volcanic centers have been discovered on Venus by Venera and

[1]Now at Seismological Laboratory, California Institute of Technology, Pasadena.

Paper number 1999JB900213.
0148-0227/99/1999JB900213$09.00

Magellan missions [*Barsukov et al.*, 1986; *Head et al.*, 1992, *McKenzie et al.*, 1992]. While some of the lineations might be caused by uplift-related faulting [e.g., *Stofan et al.*, 1992], most of them have been interpreted as dike-induced grabens [*Grosfils and Head*, 1994; *Ernst et al.*, 1995]. *McKenzie and Nimmo* [1999] suggested that even larger giant radiating dike swarms exist on Mars.

Flood magmatism (in particular, giant radiating dike swarms and associated flood basalt provinces) has been implicated in such global phenomena as continental breakups [*Morgan*, 1971, 1983] and mass extinctions [*Stothers*, 1993; *Courtillot*, 1994]. In both cases, possible relationships have been suggested on the basis of close spatial and/or temporal correlations of the events. Obviously, establishing casual links requires a thorough understanding of the dynamics of magma emplacement and its potential effect on the corresponding phenomenon (e.g., the timescale and magnitude of lithospheric weakening in the case of a continental breakup or the rate of release of volatiles into atmosphere in the case of a mass extinction). However, physical aspects of magma transport through the lithosphere during flood basalt volcanism are still poorly constrained. In this paper we review several important questions related to the emplacement of giant dike swarms and address these questions by solving the corresponding boundary value problems of heat and mass transfer.

2. Mode of Emplacement

In terrestrial giant dike swarms, published field data (e.g., magnetic anisotropy measurements, petrofabrics, dike wall structures) often indicate that the flow was predominantly vertical in the central area of the topographic uplift (e.g., within ~500 km from the swarm center for the Mackenzie swarm in Canada) but changed to horizontal farther from the center [*Greenough and Hodych*, 1990; *Ernst and Baragar*, 1992]. This suggests a transport style similar to that observed (on much smaller scales) in the volcanic rift zones of Iceland and Hawaii. That is, magma ascends from the mantle source to the level of neutral buoyancy (which can be controlled by density or rheology contrasts [see *Fialko and Rubin*, 1998]) and subsequently spreads laterally in dikes from the magmatic center down the rift zones [*Einarsson and Brandsdottir*, 1980; *Klein et al.*, 1987]. Forces available to drive the flow include an excess magma pressure p_0 at the magmatic center, a topographic slope α, and downrift variations in the dike-perpendicular stress. The driving pressure gradient due to an excess source pressure p_0 decreases with increasing dike length x_N and is of the order of p_0/x_N [*Spence and Turcotte*, 1985; *Lister and Kerr*, 1991]. Taking $x_N \sim 10^3$ km (characteristic propagation length) and $p_0 \sim 30$ MPa (consistent with observed dike widths being produced by elastic deformation, see section 3), one obtains a value of the order of 30 Pa/m. A topographic driving pressure gradient may be generated by plume-related uplift; the magnitude of the uplift is estimated to be of the order of a few kilometers [*Morgan*, 1983; *Watson and McKenzie*, 1991]. Assuming that the level of neutral buoyancy parallels the topographic slope, the driving pressure gradient due to topography is

$$G_T = \rho_m g \alpha, \tag{1}$$

where ρ_m is magma density and g is gravitational acceleration. Note that G_T is independent of dike length and constant provided α is constant. For an uplift of 2 km in 10^3 km, $\alpha = 2\times10^{-3}$, and (1) gives topographic driving pressure gradients of the order of 60 Pa/m. Variations in the horizontal tectonic stress depend on the particular distribution of loads in the lithosphere and are difficult to generalize. For extensional tectonic environments, such that the least compressive horizontal stress resides on the Mohr-Coulomb failure envelope (i.e., under conditions appropriate for normal faulting), the vertical gradient in the horizontal stress $\partial\sigma_h/\partial z$ is of the order of 13 kPa/m (assuming hydrostatic pore pressure and $\mu \sim 0.6$, where μ is the rock friction coefficient [see, e.g., *Hickman*, 1991]). Then the horizontal stress gradient corresponding to a transition from a normal faulting regime to a lithostatic stress state at depth $z \sim 10$ km (a representative brittle-ductile transition) over a lateral distance $H = 10^3$ km is of the order of $(\rho_r g - \partial\sigma_h/\partial z)z/H \sim 100$ Pa/m, where ρ_r is rock density. (Note that increases in the horizontal compression to levels greater than the vertical stress will cause dikes to rotate their planes of propagation and turn into sills; *Ernst et al.* [1995] report examples of coeval sills apparently emplaced at large distances from the source by lateral injection from giant dikes.) Thus variations in the tectonic stress may, in principle, dominate the dynamics of magma emplacement in giant dike swarms. For simplicity, we adopt a constant value of the global driving pressure gradient $G = 50$ Pa/m in most of our calculations below.

An important question is whether the magma flow during giant dike emplacement was laminar or turbulent. As has been demonstrated in earlier studies, the differences in flow regime have a profound effect on heat transfer and flow evolution [*Hulme*, 1975; *Huppert*, 1989]. If the flow was turbulent, a substantial amount of melting and assimilation of the host rock is to be expected [*Huppert and Sparks*, 1985]. Under laminar flow conditions, eventual melting of the host rocks (at much lower rates than during turbulent flow) is possible if magma erupts at some distance from the source [*Bruce and Huppert*, 1990; *Lister and Dellar*, 1996]; otherwise, melting is predicted to be limited to a small region near the source [*Fialko and Rubin*, 1998].

The flow regime is a function of the Reynolds number *Re* which characterizes the relative importance of inertial and viscous forces in the moving fluid. Assuming Newtonian rheology, *Re* depends on the dimensionless group

$$R = \frac{w_0^3 G \rho_m}{\eta^2}, \tag{2}$$

where w_0 is the characteristic dike half width, G is the driving pressure gradient, and η is the magma dynamic viscosity. For laminar and turbulent flows the corresponding Reynolds numbers Re_l and Re_t may be written as

$$Re_l = \frac{2}{3}R, \qquad Re_t = 15.4R^{4/7}. \tag{3}$$

Physically, expressions (3) represent a ratio of the two-dimensional (2-D) volume flux to the kinematic viscosity of the fluid [e.g., *Batchelor*, 1967] (also see section 6). A transition from laminar to turbulent flow is expected when Re_l exceeds ~2000. Using as an example $w_0 = 25$ m, $G = 50$ Pa/m, $\rho_m = 2{,}700$ kg/m^3, and $\eta = 100$ Pa s (basalt viscosity), from (2) and (3) one obtains $Re_l \sim O(10^5)$ and $Re_t \sim O(10^4)$; that is, the flow in dikes that are tens of meters wide and thicker must be turbulent and produce extensive thermal erosion of the country

rocks. This conclusion must be reconciled with presence of chilled margins and apparent absence of large amounts of assimilated crustal material in even the thickest dikes in giant swarms [*Mohr*, 1987; *Cadman et al.*, 1990]. Thus one must ask whether the field observations should be regarded as indicative of the laminar character of magma flow (which implies magma viscosities that are too high for supersolidus basalts [*Shaw*, 1972]) or if chilled margins and low magma contamination may somehow be consistent with turbulent magma emplacement. We shall argue in favor of the second scenario.

3. Dike Width Problem

Intrinsically related to the mode of emplacement is the question of what physical process was responsible for the exceedingly large observed dike widths. Because dikes propagate via intruding and elastically inflating preexisting or self-induced fractures, dike width is often viewed as reflecting the excess magma pressure (the difference between the magma pressure and the ambient normal stress) [e.g., *Pollard*, 1987]. While this is generally true when emplacement is thermally limited (that is, when magma freezing precedes and ultimately causes dike arrest), this assumption does not hold for dikes that melt their conduits. In the latter case, the final dike width reflects some complex interaction between the deformation of the host solid, the thermodynamics of melting/freezing at the magma-host rock interface, magma flow, and the supply characteristics of the magma source. Although in most situations the initial contact of magma and host rock results in magma freezing, subsequent evolution of the flow may give rise to remelting ("melt back") of the initial chill and thermal erosion of the original solid. Such behavior has been demonstrated theoretically for both turbulent [*Hulme*, 1975; *Huppert*, 1989] and laminar [*Bruce and Huppert*, 1990; *Lister and Dellar*, 1996] flows and has been inferred from field data [*Greenough and Hodych*, 1990; *Philpotts and Asher*, 1993].

Exceedingly large dike widths and the large number of dikes in giant radiating dike swarms, in fact, present a space problem for intrusion [*Baragar et al.*, 1996]. If dikes were emplaced by elastic inflation, their widths may be used to estimate a lower bound on the amount of extensional strain in the crust prior to dike emplacement. For radial dike swarms, this bound is given by the ratio of the cumulative dike thickness along some arc centered at the focus of the swarm to the arc length. *Baragar et al.* [1996] report that corresponding "elastic" strains associated with emplacement of the Mackenzie dikes are of the order of 1.7×10^{-2} (3 km of cumulative dike width in 180 km of arc) and 4.2×10^{-3} (1.7 km in 392 km) at distances of 400 and 900 km from the inferred uplift center, respectively. Given that the maximum circumferential strain provided by the topographic uplift is $O(\alpha^2)$ [e.g., *Landau and Lifshitz*, 1986], it follows that elastic accommodation of the Mackenzie swarm would require unrealistically large uplifts. *Baragar et al.* [1996] suggested that a superimposed regional tectonic stress could provide some additional extension. However, the magnitude of such extension was unlikely to exceed the one due to the topographic doming itself. This is because the radial pattern of the swarm is essentially unperturbed within ~1000 km from the inferred uplift center, implying that a complementary extension (if any) must have had nearly axisymmetric nature. We point out that the problem of space may be removed if some fraction of the Mackenzie dikes was emplaced by a nondilational mechanism.

That the aperture of at least some giant basaltic dikes was produced by a process other than elastic dilation was demonstrated by field observations long ago. For example, on the basis of a study of the crosscutting relationships of the Medford dike in eastern Massachusetts, *Billings* [1925] concluded that the dike was not emplaced by mechanical separation of the wall rock due to the excess magma pressure (see Figure 1a). In particular, he observed that some of the earlier dikes crossing the Medford dike at various angles have no along-strike offsets, while others appear to be terminated by the giant dike (e.g., dikes K and P in Figure 1a), implying that the latter was formed mainly by replacing (not displacing) the host rocks. Similar structural relationships were observed by *Bridgewater and Coe* [1970] for several giant dikes in Isortoq, south Greenland. Figure 1b shows an example of one of the Isortoq dikes crosscut by an older basaltic dike (marked as BDo in Figure 1b). One can see that the cross dike is not only not offset by the younger giant dike but also protrudes into the latter by as much as several tens of meters forming a so-called "bridge" [*Bridgewater and Coe*, 1970]. Note that separation of the protruded segments of the cross-dike provides an upper bound on the amount of dilation associated with emplacement of the giant dike, which is about one third of the total dike width in the case shown in Figure 1b. Both *Billings* [1925] and *Bridgewater and Coe* [1970] suggested that magma stoping was a primary mechanism for generating the observed dike widths. Magma stoping has been appealed to in other cases when field evidence pointed out to a nondilatational character of giant dike emplacement [e.g., *Upton*, 1974]. However, stoping has been traditionally rejected as a dike-forming mechanism because of the nominally regular sheet-like form of (even the largest) dikes and the usual absence of xenoliths [*Richardson*, 1923]. We propose that thermal erosion is a more likely mechanism for generating the inferred nondilatant emplacement of giant dikes. For example, the existence of bridges (Figure 1b) may be readily interpreted in terms of differences in the melting temperature between different units comprising the host rocks. In particular, more refractory basaltic cross dikes are likely to be more resistant to assimilation than the felsic country rocks. As we demonstrate below, magma contamination due to massive melting and assimilation of crustal material during giant dike emplacement may be quite small (of the order of several percents), in reasonable agreement with geochemical data. We shall return to the discussion of field evidence for thermal erosion in section 7.

The conclusion that the observed giant dike thicknesses were unlikely to be produced by elastic deformation also follows from theoretical arguments. Assuming that the dike width is controlled by the excess magma pressure alone, one may estimate the latter using analytical solutions for a 2-D crack in an infinite elastic body [see, e.g., *Lister*, 1990; *Khazan and Fialko*, 1995]. For a dike trapped at the level of neutral buoyancy (LNB), assuming a linear excess pressure distribution with depth and negligible rock fracture resistance, one obtains [*Fialko and Rubin*, 1998]

$$p_0 = \frac{2}{\pi^{1/2}}\left(w_0 MV\right)^{1/2}, \qquad (4)$$

where p_0 is the excess magma pressure at the dike center, M is the elastic stiffness of the host rock, w_0 is the dike half width

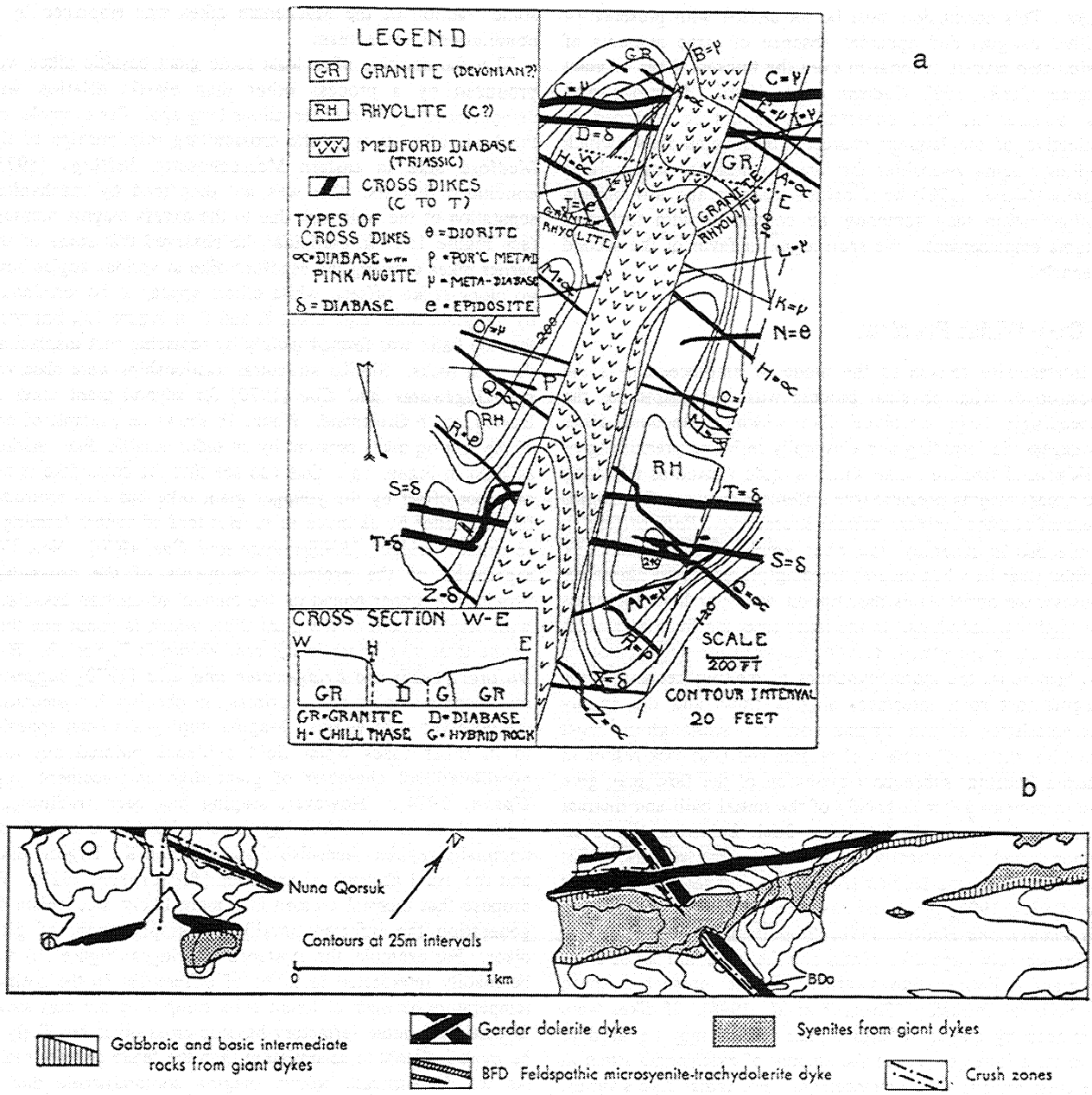

Figure 1. (a) The Medford dike in eastern Massachusetts. From *Billings* [1925], reproduced by permission of the Chicago University Press. Older lineaments cut by the dike appear to continue with no offsets in their own planes, implying that the host rock between the dike walls has been replaced by the magma. Billings proposed "large-block stoping" as the cause of the removal of the crustal material. We would suggest that this removal was accomplished by thermal erosion. (b) The Isortoq (stippled) and Gardar (solid) dikes near Isortup sarfa, south Greenland. From *Bridgewater and Coe* [1970], reproduced by permission of John Wiley & Sons Ltd. The Gardar dike striking at 110° (denoted as BDo in Figure 1b) partially survives as a "bridge" after being cut by a younger giant dike. The existence of a bridge is a compelling evidence for nondilational emplacement of the giant dike (see text for details).

at the center (see Figure 3), and V is the vertical gradient in the excess magma pressure. For the LNB due a to density step $\Delta\rho$ = 600 kg/m^3, with the magma density being intermediate between the rock densities above and below the LNB, V = $0.5\Delta\rho g$ ~3 kPa/m. Adopting w_0 = 25 m and M = 10 GPa as representative values, from (4) one obtains an excess pressure at the dike center of the order of 30 MPa, greatly exceeding the rock tensile strength. Assuming that the rock tensile strength is a measure of the excess pressure required for dike initiation and if the stress state in the crust prior to dike intrusion is lithostatic, this implies that the excess pressure at the source was increasing after the dike initiation, which is unlikely. In addition, these parameters give rise to a dike half height $h = (\pi w_0 M/V)^{1/2}$ ~15 km [*Fialko and Rubin*, 1998], i.e., to a level of neutral buoyancy that is too deep, given the density contrast assumed above. Reasonable variations in the constitutive parameters in (4), as well as in the particular form of the excess magma pressure distribution with depth, do not

substantially alter the conclusion that the observed dike thicknesses in giant dike swarms seem to be too large to be explained by elastic inflation alone if the level of neutral buoyancy was controlled by density contrasts between the magma and the host rocks.

For a dike trapped at a rheological step in the presence of tectonic extension, the vertical gradient in excess magma pressure V in the upper part of the dike (i.e., above the brittle-ductile transition) is given by the difference between $\rho_m g$ and the rock failure envelope; for $\mu \sim 0.6$ we obtain $V \sim 14$ kPa/m and from (4) we obtain $p_0 \sim 60$ MPa. While the inferred excess pressure is even higher than in the previous example, it cannot be ruled out on physical grounds. However, in many cases, there are no indications that tectonic extension preceded flood volcanism [*Hooper*, 1990; *Duncan and Richards*, 1991; *Hill et al.*, 1992]. Note that if large dike thicknesses observed in the field are interpreted as reflecting high excess magma pressures, this implies that the excess pressure (and concomitant driving pressure gradient p_0/x_N, of the order of 30 Pa/m, as estimated in section 2) was high at the time of the termination of flow. The results of sections 4 and 5 indicate that giant dikes with even substantially lower driving pressure gradients are in no danger of freezing during emplacement. Thus, causing dike arrest in such cases would require the horizontal stress to increase at a rate that cancels both the ~30 Pa/m that comes from the excess pressure and the ~60 Pa/m likely to come from topography. Therefore we conclude that consideration of mechanisms other than elastic opening that might generate the observed dike widths is certainly warranted.

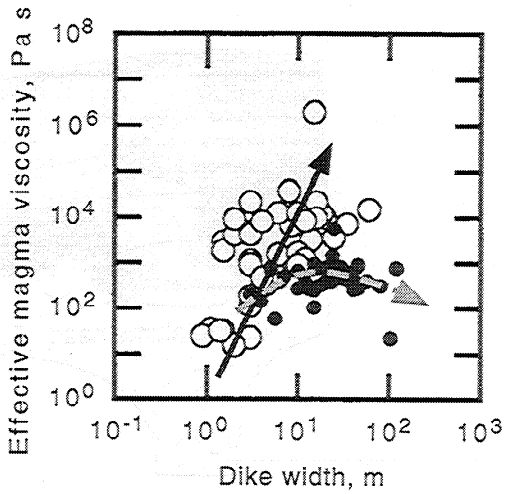

Figure 2. Relationships between magma viscosity and dike width observed in the field. Open circles correspond to a selection of dikes from Japan and South America. Solid arrow denotes a trend $w^4 \propto \eta$ indicative of thermally limited dike emplacement [*Kerr and Lister*, 1995]. Solid circles and dashed arrow correspond to dikes associated with flood basalt volcanism. Data are taken from *Wada* [1994].

4. Source Conditions and Flow Termination

Our calculations below indicate that giant dike emplacement was not thermally limited (that is, dike freezing followed rather than preceded the termination of flow). This conclusion is also apparent from empirical correlations between dike width and magma viscosity established for large numbers of dikes worldwide. Figure 2 shows an example of one such correlation [*Wada*, 1994]. As may be seen in Figure 2, dikes that are not associated with flood volcanism in general exhibit a trend compatible with $w^4 \propto \eta$, which can be argued to be characteristic of thermally limited dike emplacement [*Kerr and Lister*, 1995]. In contrast, dikes comprising giant dike swarms follow a quite different pattern, in which the dike thickness is nearly independent of the magma viscosity. For dikes that are not thermally limited, the mechanism responsible for flow arrest was most likely related to eventual depletion of the magma source.

There are two possible scenarios of magma supply during giant dike intrusion. The first implies the existence of a large shallow magma chamber periodically replenished by melt from the mantle source. When the excess pressure in the chamber is sufficient to exceed the chamber strength, lateral dike intrusion is initiated. If the chamber volume is large enough compared to the dike volume, the excess magma pressure at the dike source may be considered essentially constant (the so-called "buffered" condition in the terminology of *Parfitt and Head* [1993]). In the second scenario, dikes propagate directly from the mantle source to the level of neutral buoyancy, at which they start to spread laterally. In this case the dike "source" is effectively a region of transition from vertical to horizontal flow, and the excess pressure at this source may vary with time. Geochemical data indicate that the Mackenzie magmas equilibrated at low pressures, which implies the presence of one (or more) high-level magma chambers [*Kretz et al.*, 1985; *Gibson et al.*, 1987]. On Venus, where erosion does not obliterate surface structures associated with plume-related swarms, observations have been interpreted as suggesting the presence of shallow, relatively equidimensional reservoirs feeding giant dikes [*Ernst et al.*, 1995]. In order to simplify the problem and to get some qualitative insight into the flow behavior, hereafter we assume that emplacement occurs under conditions of nearly constant source pressure. In this case, and if the dominant driving pressure gradient does not vary substantially along the propagation path (see section 2), the elastic dike width and height are expected to be relatively constant along strike [*Fialko and Rubin*, 1998, 1999]. When a dike propagates out of the topographic swell, a decrease in the topographic driving pressure gradient is expected to cause a decrease in the dike propagation velocity and a concomitant increase in the local excess magma pressure, making the dike wider and taller (Figure 3). If the level of neutral buoyancy does not deepen with respect to the surface away from the swell, at this point the dike would be most likely to erupt. Indeed, many flood basalts appear to have erupted on the periphery of the inferred topographic uplifts [e.g., *Gill et al.*, 1992; *Ernst and Buchan*, 1997].

For constant source pressure conditions, a constant global driving pressure gradient along the dike, and a specified magma viscosity, the only parameter controlling the magma flux is the dike width. Increases in width due to thermal erosion will cause a corresponding increase in magma flux. Eventually, enough magma is bled off by the dike that the excess pressure at the source will decrease. However, this decrease may not be sufficient to close the dike if by this time there has been a large amount of melt back. Ultimately, the flow will stop when the pressure at the magma source equals that at the base of a hydrostatic column of magma extending from the source to the eruption site. For eruption at the margin

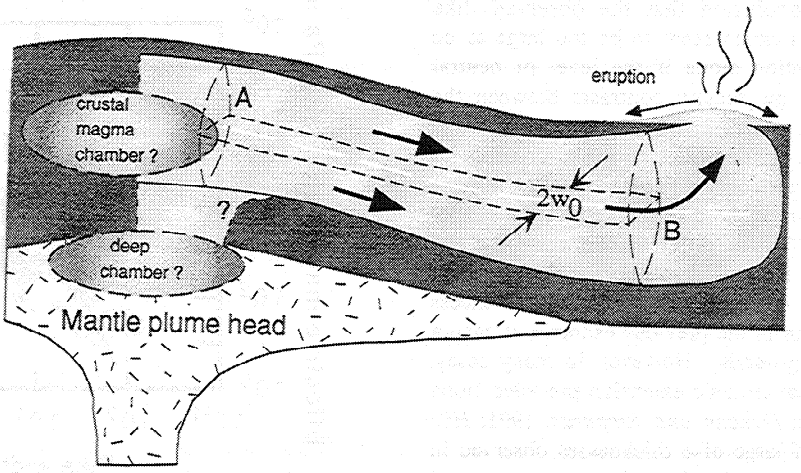

Figure 3. Giant dike propagating along the level of neutral buoyancy (white dashed line) down the slope produced by a buoyant plume head. The magma source might be at or below the level of neutral buoyancy. When the topographic slope levels off, continuity of magma flux requires that the dike increases its cross-sectional area. In the absence of along-strike variations in the dike-perpendicular stress, and if the level of neutral buoyancy parallels the topography, at this point the dike is most likely to erupt. Solid arrows denote general directions of magma flow.

of a topographic swell of 2 km, this corresponds to magma underpressure at the source (relative to the lithostatic stress) of ~50 MPa, which may be sufficiently large to cause extensional collapse, or implosion, of the shallow magma plumbing system. If the shallow magma chamber is connected to the source region in the mantle, the pressure drop will eventually be transferred there, which may promote additional pressure-release melting. Our final aim is to constrain the postemplacement processes by comparing predictions of our theoretical model to the field observations. Reconstructing the mechanisms that terminated magma flow is particularly important because the field data mainly record the final stages of dike emplacement.

5. Thermally Admissible Dike Width

We proceed by determining the minimum dike width that would enable a dike to transport magma over the observed propagation distances without freezing. Heat sources available to retard solidification include the latent heat of crystallization, magma superheat (if the initial magma temperature exceeds some effective solidus), and shear heating (viscous dissipation). In a propagating dike, magma superheat and latent heat are lost over a distance known as the "thermal entry length" [e.g., *Fedotov*, 1978; *Delaney and Pollard*, 1982]; if viscous dissipation is negligible, beyond this distance magma completely solidifies [*Fialko and Rubin*, 1998]. For sufficiently large fluid velocities, however, shear heating may be strong enough to keep the magma liquid beyond the thermal entry length, or even surpass the conductive heat loss, giving rise to "thermal runaway" (unbounded propagation accompanied by melt back of the channel walls). We performed numerical experiments to establish the range of geophysical parameters for which viscous dissipation would prevent dikes from freezing.

Consider the 2-D flow of incompressible magma into a parallel-walled channel having infinite extent in the flow direction and an initial width of $2w_0$ (Figure 4). The flow is driven by a constant global pressure gradient G (the local pressure gradient in the magma is allowed to vary along the flow direction to accommodate variations in the channel aperture caused by magma freezing and/or channel wall melting [*Fialko and Rubin*, 1998]). At time $t = 0$, magma enters the channel at the inlet ($x = 0$) having uniform temperature T_m. The initial temperature of the ambient solid ($y > |w_0|$) is T_0. For simplicity, we assume that the magma and host rocks differ only by phase and are characterized by a common freezing/melting temperature T_s, latent heat of crystallization/fusion L, thermal diffusivity κ, and specific heat capacity c. The magma is supposed to be sufficiently viscous and the channel sufficiently narrow that the flow is laminar and the lubrication approximation applies. The magma velocity is sufficiently high that along-stream conduction in the magma is negligible compared to along-stream advection [e.g., *Delaney and Pollard*, 1982; *Bruce and Huppert*, 1990]. Conservation of energy in the fluid is given by

$$\rho_m c \frac{\partial T}{\partial t} = k \frac{\partial^2 T}{\partial y^2} - \rho_m c \mathbf{u} \cdot \nabla T + \eta D \,, \qquad (5)$$

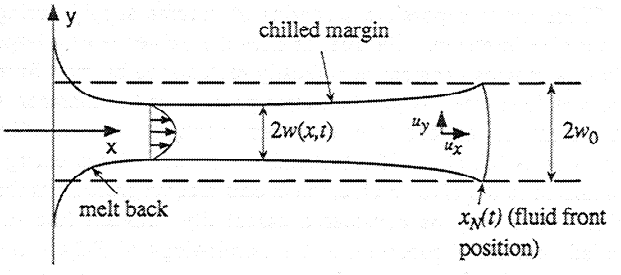

Figure 4. A semi-infinite parallel-walled channel is filled by hot viscous fluid supplied at $x = 0$. Geometry of the fluid-occupied portion of the channel is governed by the processes of crystallization/melting at the phase boundary (curved solid line). From *Fialko and Rubin* [1998].

where $T = T(x,y,t)$ is fluid temperature, t is time, k is thermal conductivity ($k \equiv \kappa\rho_m c$), $\boldsymbol{u} = \{u_x, u_y\}$ is the fluid velocity vector, and D is the dissipation function [e.g., *Bird et al.*, 1960],

$$D = \left(\frac{\partial u_x}{\partial y} + \frac{\partial u_y}{\partial x}\right)^2 + 2\left(\frac{\partial u_x}{\partial x}\right)^2 + 2\left(\frac{\partial u_y}{\partial y}\right)^2. \quad (6)$$

A small cross-stream component of the fluid velocity u_y results from the along-stream variations in the channel thickness due to freezing/melting at the phase boundary; for small variations in the channel thickness (which is the case along most of the channel), D is dominated by cross-channel variations in the along-stream velocity, $D \approx (\partial u_x/\partial y)^2$. Equation (5) states that changes in the fluid temperature at a given position are governed by the balance between the cross-stream heat conduction (first term on the right-hand side of (5)), advection of heat by the moving fluid (second term), and internal heat generation due to viscous dissipation (third term). Note that u_y cannot be neglected in the advective term because it gets multiplied by large cross-stream temperature gradients. We assume the fluid to be isoviscous; this approach is conservative as far as the conditions for thermal runaway are concerned, as corroborated by our calculations using temperature-dependent magma viscosity (unpublished results). In the solid, heat transfer is by diffusion only, and conservation of energy is given by

$$\rho_m c\frac{\partial T}{\partial t} = k\frac{\partial^2 T}{\partial y^2}. \quad (7)$$

We nondimensionalize the variables in (5) and (7)

$$\chi = \frac{x}{\hat{x}}, \quad \psi = \frac{y}{\hat{y}}, \quad \tau = \frac{t}{\hat{t}} \quad (8a)$$

with respect to the scales

$$\hat{x} = \frac{w_0^4 G}{\kappa\eta}, \quad \hat{y} = w_0, \quad \hat{t} = \frac{w_0^2}{\kappa}, \quad (8b)$$

where w_0 is the initial channel half width, $\hat{t}$ is the thermal diffusion timescale, and $\hat{x}$ is a thermal entry length given (up to a premultiplying constant) by the product of $\hat{t}$ and the average fluid velocity in the absence of freezing [*Fedotov*, 1978; *Delaney and Pollard*, 1982; *Fialko and Rubin*, 1998]. A nondimensional temperature θ is defined by

$$\theta = \frac{T - T_0}{T_m - T_0}. \quad (9)$$

Upon nondimensionalization using (8) and (9), equations (5) and (7) become

$$\frac{\partial\theta}{\partial\tau} = \frac{\partial^2\theta}{\partial\psi^2} - \boldsymbol{u}\cdot\nabla\theta + Br\sigma^2, \quad (10)$$

$$\frac{\partial\theta}{\partial\tau} = \frac{\partial^2\theta}{\partial\psi^2}, \quad (11)$$

respectively, where σ is the dimensionless shear stress in the fluid and Br is the Brinkman number,

$$Br = \frac{w_0^4 G^2}{\eta k\left(T_m - T_0\right)}. \quad (12)$$

For laminar flow the along-stream component of the fluid velocity vector $\boldsymbol{u}$ is given by plane Poiseuille flow,

$$u_\chi = -\frac{1}{2}\left(\omega^2 - \psi^2\right)\gamma, \quad (13)$$

where $\omega = w/w_0$ is the nondimensional channel half width available for flow (i.e., initial half width minus chilled margin) and γ is the local driving pressure gradient (in units of G). The local driving pressure gradient γ is related to the global volume flux (per unit height) q as

$$\gamma = -\frac{3}{2}\frac{q}{\omega^3}. \quad (14)$$

Because for the rigid-wall channel the volume flux q (as well as the Reynolds number Re) is independent of the position along the channel [*Lister and Dellar*, 1996; *Fialko and Rubin*, 1998], local decreases in the channel aperture due to freezing result in increases in the local driving pressure gradient γ and fluid velocity u_χ (inversely, melt back decreases γ and slows the flow locally). Integrating (14) from the origin to the current position of the fluid front $x_N(\tau)$ (Figure 4) and noting that the global driving pressure gradient is -1 with scalings (8), one may obtain the following expression for q:

$$q(\tau) = \frac{2}{3}x_N(\tau)\left(\int_0^{x_N(\tau)}\frac{d\chi}{\omega^3(\chi,\tau)}\right)^{-1}. \quad (15)$$

The cross-stream component of the fluid velocity u_ψ can be obtained from (13) using local continuity, and for the rigid-walled channel it is [*Lister and Dellar*, 1996]

$$u_\psi = \frac{\psi}{\omega}\frac{\partial\omega}{\partial\chi}u_\chi. \quad (16)$$

The shear stress σ associated with plane Poiseuille flow is $\sigma = \partial u_\chi/\partial\psi = \psi\gamma$. The local rate of migration of the solid-liquid interface is governed by the Stefan condition

$$S\frac{\partial\omega}{\partial\tau} = \left.\frac{\partial\theta}{\partial\psi}\right|_{\psi=\omega-}^{\psi=\omega+}, \quad (17)$$

where the right-hand side denotes the jump in the temperature gradient across the solid-liquid interface, $f|_a^b = f(b) - f(a)$, and S is the Stefan number,

$$S = \frac{L}{c\left(T_m - T_0\right)}. \quad (18)$$

At the phase boundary ($|\psi| = \omega(\chi,\tau)$) the temperature equals the dimensionless freezing temperature Θ,

$$\Theta = \frac{T_s - T_0}{T_m - T_0}. \quad (19)$$

The flow evolution is governed by three nondimensional groups: the Brinkman number Br (equation (12)), the Stefan number S (equation (18)) and the dimensionless freezing temperature Θ (equation (19)). We wish to calculate the critical values of the Brinkman number $Br_c(S, \Theta)$ which demarcate the regime of ultimate solidification from that of thermal runaway.

The system (10)-(11) was solved numerically using a finite difference scheme that is second order in both space and time (for details, see *Fialko and Rubin* [1998]). The accuracy of the numerical code was checked by conservation of energy, by mesh and time step refinements, and by comparison with a few available asymptotic solutions. Thus, in the absence of freezing ($S \to \infty$), our algorithm accurately converges to the analytical solution $\theta(\psi) = \Theta + Br(1-\psi^4)/12$ for the steady state temperature distribution due to viscous dissipation in a

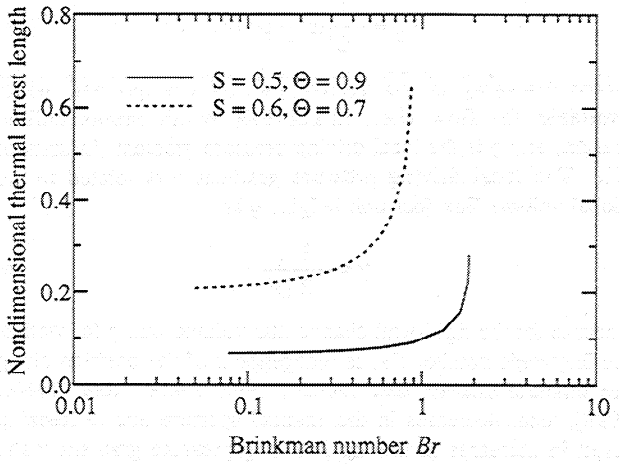

Figure 5. Nondimensional thermal arrest distances for flow in a rigid-walled slot as a function of the Brinkman number for different values of the dimensionless freezing temperature Θ and Stefan number S.

flat channel with isothermal walls [e.g., *Holman*, 1997]. A nondimensional thermal arrest length x_N^* (the flow length at which the flow becomes completely blocked by solidification) was found by solving the system (10)-(11) for given values of S and Θ. The dependence of the thermal arrest length on the Brinkman number Br is shown in Figure 5. As may be seen from Figure 5, the onset of thermal runaway is quite sharp and for practical purposes may be approximated by a step function,

$$x_N^* = \begin{cases} x_{0N}^*, & w_0 < w_{0c} \\ \infty, & w_0 \geq w_{0c} \end{cases},$$

where x_{0N}^* is the nondimensional thermal arrest length in the limit of negligible viscous dissipation [*Fialko and Rubin*, 1998] and w_{0c} is the critical dike half width that corresponds to the onset of thermal runaway. Rewriting (12), one obtains

$$w_{0c} = \left(Br_c(S,\Theta) \frac{k\eta(T_m - T_0)}{G^2} \right)^{1/4}. \qquad (20)$$

The dependence of Br_c on the dimensionless freezing temperature Θ is shown in Figure 6 for several values of the Stefan number S. As one might expect, the runaway occurs when Br is of the order of unity. Assuming G = 50 Pa/m, k = 2.7 W/(m °C), T_m = 1250 °C, η = 50 Pa s [e.g., *Shaw*, 1972], and T_0 = 250 °C, from (20) we find that dikes thicker than ~7 m will not be in danger of freezing at any distance from the source provided the driving pressure gradient G does not decrease. Note that given the assumed values of η and G, this thickness satisfies our initial assumption of laminar flow (equations (2) and (3)). It should be mentioned that the thermal arrest length of a 7-m-wide dike (for the same parameters as used above) is $O(10^3)$ km even in the absence of viscous dissipation, coincidentally of the same order as the observed propagation distances of giant dikes. This implies that both heat advection from the magma source and viscous dissipation may be appreciable over the observed propagation distances, and for dikes that ultimately erupt, estimate (20) in fact gives an upper bound on the minimum thermally admissible dike width.

6. Turbulent Melt Back

Section 5 shows that dike thicknesses <10 m are sufficient for dikes to propagate thousands of kilometers without freezing. After propagating beyond the topographic swell caused by a mantle plume the dike slows down and builds up excess pressure near the leading edge, which may cause it to erupt (Figure 3). We investigate the further thermal evolution of such a dike by approximating the flow in a horizontal cross section through the dike middle by a finite channel model in which the magma is supplied to the channel inlet (point A in Figure 3) and flows out of the channel (e.g., erupts onto the surface) at a specified distance H from the inlet (point B in Figure 3). The reduction in the driving pressure gradient caused by increases in the excess magma pressure at the outlet is assumed to be small compared to the total driving pressure gradient (e.g., due to the topographic slope). A continual magma supply ensures that sufficiently wide dikes will experience eventual melting along their entire length, in the fashion predicted by *Bruce and Huppert* [1990] and *Lister and Dellar* [1996]. As the magma flux increases as a result of melt back, a concomitant increase in the Reynolds number may result in Re exceeding ~2000, causing the flow to become turbulent. From (2)-(3), this width is estimated to be ~11 m for G = 50 Pa/m and η = 50 Pa s. Feedback between viscous heating and temperature-dependent magma viscosity may result in the onset of turbulence in dikes that are thinner still [*Fujii and Uyeda*, 1974; *Hardee and Larson*, 1977].

In turbulent flow the heat transfer from the magma to the host rock is no longer dominated by molecular diffusion but involves substantial cross-stream advection by eddy currents, which greatly enhances heat loss from the magma [*Kutateladze*, 1963; *Holman*, 1997]. Figure 7 shows schematic temperature profiles across the channel for laminar and turbulent flows. Neglecting the fluctuating temperature component, the core of the fully developed turbulent flow may

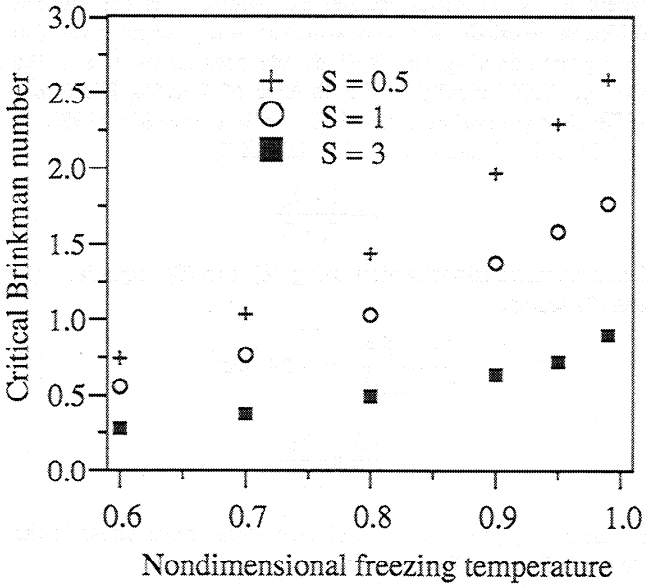

Figure 6. Values of the critical Brinkman number Br_c (i.e., above which viscous dissipation would allow for infinite flow) calculated for a range of the dimensionless freezing temperatures Θ and Stefan numbers S.

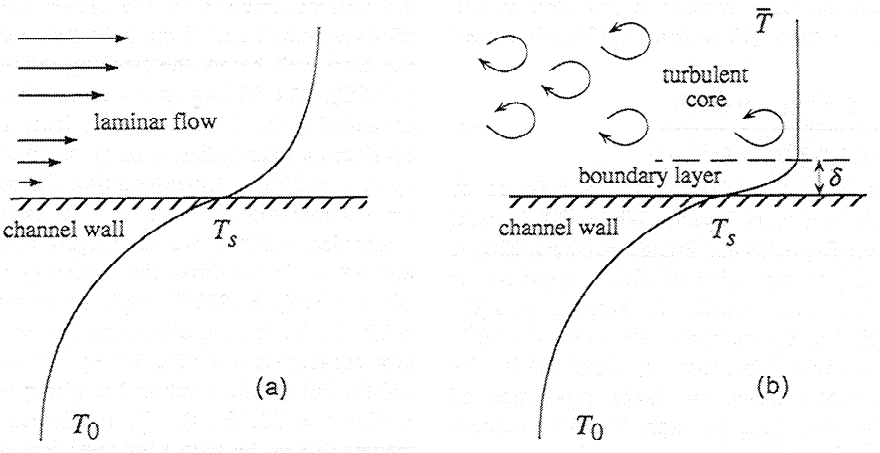

Figure 7. Temperature profiles characteristic of heat transfer during (a) laminar and (b) turbulent flow. In laminar flow, temperature profile is governed by a balance between along-stream advection and across-stream conduction. In turbulent flow, eddy currents result in significant cross-stream advection, greatly increasing heat loss from the magma to the ambient rocks.

be considered essentially isothermal because of thorough convective mixing; most temperature changes are confined to a thin boundary layer near the dike wall. The physically significant parameter in the case of turbulent flow is the bulk, or "mixing cup" temperature

$$\overline{T}(x,t)=\frac{1}{w(x)}\int_0^{w(x)} T(x,y,t)dy. \qquad (21)$$

For magmas characterized by large Prandtl numbers, $Pr \equiv \eta/\kappa\rho_m >> 1$, the thermal boundary layer is contained within the mechanical (laminar) boundary layer along the channel wall and is much smaller than the channel width. In this case, the conservation equation (5) can be integrated over the channel width to produce an energy balance equation for the bulk temperature $\overline{T}$ (see the appendix for details),

$$\frac{\partial\overline{T}}{\partial t}+\frac{1}{w}\frac{\partial w}{\partial t}\left(\overline{T}-T_s\right)=\frac{\kappa_e}{w}\left.\frac{\partial T}{\partial y}\right|_{y=w}-\frac{Q}{2w}\frac{\partial\overline{T}}{\partial x}+\frac{Q}{2w\rho_m c}\frac{\partial p}{\partial x}, \qquad (22)$$

where κ_e is effective thermal diffusivity of magma that accounts for the cross-stream advection of heat, $\partial T/\partial y$ is the temperature gradient at the wall that depends on the structure of the thermal boundary layer in the fluid, Q is the volume flux in the channel per unit height, $\partial p/\partial x$ is the local driving pressure gradient, and the viscous dissipation term (last term on the right-hand side) is evaluated based on the total rate of work done on the fluid to compensate viscous pressure losses. For turbulent flows the dependence of Q on the dike width and the driving pressure gradient must be derived from empirical laws. We adopt the following simple relationship [*Hirs*, 1974; *Lister*, 1990]:

$$Q=15.4\left(\frac{w^{12}}{\eta\rho_m^3}\right)^{1/7}\left|\frac{\partial p}{\partial x}\right|^{4/7}. \qquad (23)$$

The Reynolds number is given by

$$Re_t=\frac{Q\rho_m}{\eta}. \qquad (24)$$

Substituting (23) into (24) and using w_0 and G as characteristic values for the channel thickness and the driving pressure gradient, one obtains expression (3) given in section 2. Introducing nondimensional variables

$$\chi=\frac{x}{H},\ \overline{\theta}=\frac{\overline{T}-T_0}{T_m-T_0},\ \psi=\frac{y}{w_0},\ \tau=\frac{\kappa t}{w_0^2},\ \omega=\frac{w}{w_0}, \qquad (25)$$

where H is the channel length, from (22) we obtain

$$\frac{\partial\overline{\theta}}{\partial\tau}=-\frac{\overline{\theta}-\Theta}{\omega}\left(\frac{Nu}{2\omega}+\frac{\partial\omega}{\partial\tau}\right)-Pe_t\overline{u}_\chi\frac{\partial\overline{\theta}}{\partial\chi}+Br_t\overline{D}. \qquad (26)$$

In (26), Pe_t and Br_t are the turbulent Peclet and Brinkman numbers,

$$Pe_t=\frac{w_0^4 G}{\kappa\eta HR^{3/7}},\qquad Br_t=\frac{Br}{R^{3/7}},$$

where R and Br are given by (2) and (12), respectively. The Nusselt number Nu is a dimensionless heat transfer coefficient relating the heat flux at the dike wall to the difference between the bulk fluid temperature and the wall (i.e., freezing) temperature [e.g., *Holman*, 1997],

$$\left.\frac{\partial\overline{\theta}}{\partial\psi}\right|_{\psi=\omega-}=Nu\left(\overline{\theta}-\Theta\right). \qquad (27)$$

The average nondimensional along-stream velocity $\overline{u}_\chi$ and viscous dissipation function $\overline{D}$ in (26) equal, correspondingly,

$$\overline{u}_\chi=7.7\frac{\overline{q}^{4/7}}{\omega},\qquad \overline{D}=\overline{u}_\chi\frac{\overline{q}}{\omega^3}, \qquad (28)$$

where $\overline{q}$ is a modified dimensionless flux,

$$\overline{q}=\left(\int_0^1\frac{d\chi}{\omega^3}\right)^{-1}, \qquad (29)$$

and $\overline{q}/\omega^3$ is a nondimensional local pressure gradient (see equation (14) and the appendix).

A dependence of the Nusselt number on the flow dynamics and the thermophysical properties of the fluid may be established from empirical data. A good fit to experimental

measurements of turbulent heat transfer is provided by the modified Petukhov's formula [*Gnielinski*, 1976; *Kays and Crawford*, 1993]

$$Nu = \frac{(\xi/8)(Re_t - 1000)Pr}{1 + 12.7(\xi/8)^{1/2}(Pr^{2/3} - 1)}, \quad (30)$$

where ξ is the drag coefficient (essentially, a measure of friction in the turbulent boundary layer). While (30) is valid over a wide range of the Reynolds and Prandtl numbers, $2300 < Re_t < 10^6$, $1 < Pr < 10^3$, extrapolation of (30) is required for treatments of turbulent heat transfer in basaltic magmas characterized by high Prandtl numbers, $Pr \sim O(10^3 - 10^5)$. Using the relation $\xi = 0.3 Re_t^{-1/4}$ proposed by *Dean* [1978] for flows in planar channels based on large quantities of experimental data, in the limit of high Prandtl numbers equation (30) may be written as

$$Nu = 0.02(Re_t - 1000) Re_t^{-1/8} Pr^a, \quad (31)$$

where a is a numerical constant. In our calculations we use $a = 0.25$, somewhat smaller than $a \sim 1/3$ suggested by (30), to account for physical damping of the turbulent heat flux in the immediate vicinity of the wall for high Prandtl numbers [*Kutateladze*, 1963; *Petukhov and Polyakov*, 1988].

The transition from laminar to turbulent flow is taken to occur when the turbulent Reynolds number exceeds 2.3×10^3, i.e., when the empirical relationships given above become applicable. In the turbulent mode the Stefan condition (17) is modified such that the temperature gradient at the dike wall from the magma side becomes (27). Within the solid the temperature is assumed to obey the 1-D diffusion equation, and the conductive profile is calculated there as previously.

In order to account for variations in host rock composition we perform calculations for several "typical" host rock compositions. In the first case, corresponding to a mafic crust, we use an effective freezing/fusion temperature T_s = 1150°C appropriate for basalt [e.g., *Bruce and Huppert*, 1990]. In the second case, corresponding to basalt intrusion into sialic crust, the situation is more complex since the freezing temperature of basaltic magma may be substantially higher than the melting temperature of the host rocks, and our assumption of a "one-component/two-phase" system is not strictly valid. In nature, such a situation may result in a "jelly sandwich" structure consisting of liquid magma/chilled basalt/melting host rock/solid host rock [*Huppert*, 1989]. To avoid consideration of the removal of the basaltic chill by the flowing magma, we adopt a common solidification/melting temperature for the magma and host rock of T_s = 850°C. This temperature may be somewhat higher than the melting temperature of granite, which may underestimate the amount of melting. By assuming that the host rock has the viscosity of basalt (upon melting), we overestimate the flux and the concomitant melt back. The latter effect is relatively minor if the volume fraction of the assimilated crustal material is relatively small and if the bulk temperature of the flow does not drop well below the freezing temperature of basalt (i.e., 1150°C). As follows from our calculations, these conditions are satisfied for dikes that are thicker than ~20 m. We also consider an intermediate case of "andesitic" crust characterized by T_s = 1050°C. Corresponding thermophysical parameters are summarized in Table 1. To explore a range of fluid mechanical regimes, we use magma viscosities of 10, 50, and 200 Pa s. In all cases the incoming magma temperature is taken to be T_m = 1250°C, the initial host rock temperature is T_0 = 250°C, the thermal diffusivity is $\kappa = 10^{-6}$ m^2/s , the specific heat capacity is $c = 10^3$ J K^{-1} kg^{-1}, the dike length is 10^3 km, and the initial dike width is 7 m (for η = 10 and 50 Pa s) or 15 m (for η = 200 Pa s). To mimic realistic decreases in the magma flux as the source becomes depleted, we enforce a linear drop in the global driving pressure gradient G from 50 Pa/m to zero over a time interval of 3 days after the dike width at the outlet exceeds 90 m.

Figure 8 shows the time evolution of the channel width at the outlet and the Reynolds number for magma flow in "granitic" host rock for η = 50 Pa s. Initial freezing of the channel is reversed several days after flow initiation, and laminar melt back eventually occurs along the whole channel. After ~50 days the Reynolds number exceeds the critical value, and flow becomes turbulent. Figure 9 shows the time dependence of the melt back rate at the channel outlet for the same simulation. The spike in the melting rate curve corresponds to the transition to turbulence and reflects the instantaneous mixing of the hot laminar core and advection of high-temperature magma from the core to the wall (in nature, magma mixing is likely to occur more gradually as the Reynolds number increases, and the melting rate variations may be smoother). After the onset of turbulence the bulk temperature of the magma along the channel drops dramatically due to enhanced heat loss and host rock melting upstream. However, as melt back proceeds and the channel width increases, so does the thermal entry length, and the bulk temperature downstream eventually goes up again. As one can see from Figure 9, melt back rates in the turbulent regime are of the order of meters per day, and the increase in dike thickness from 7 to 100 m occurs on a timescale of a few months. For an initial dike width in excess of 10 m (or magma viscosity <50 Pa s) the flow would be turbulent from the beginning and a tenfold increase in dike thickness would occur in less than a month. Calculated melting rates in the turbulent regime reveal a good match with 1-D steady state solutions [e.g., *Huppert*, 1989],

$$\frac{\partial \omega}{\partial \tau} = \frac{Nu}{2\omega} \frac{\bar{\theta} - \Theta}{S + \Theta}, \quad (32)$$

which justifies the use of a steady-state approximation for

Table 1: Thermophysical parameters used in numerical experiments

	Granite	Andesite	Basalt
Freezing temperature T_s, °C	850	1050	1150
Latent heat L, kJ/kg	300	400	500
Stefan number S	0.3	0.4	0.5
Dimensionless freezing temperature Θ	0.6	0.8	0.9

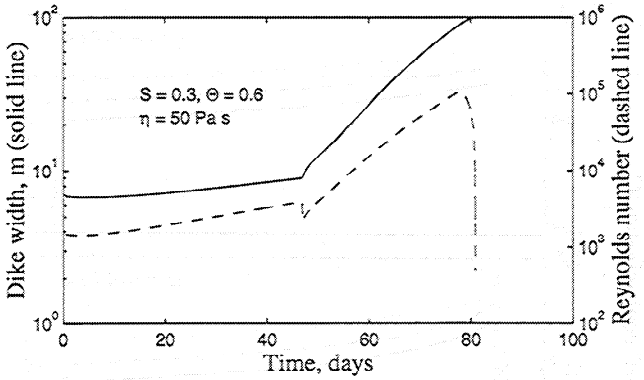

Figure 8. Time evolution of the Reynolds number (right axis, dashed curve) and the channel width at the outlet (left axis, solid curve) for flow of basaltic magma in "granitic" crust. Constant magma viscosity of 50 Pa s is assumed in this simulation. A decrease in the Reynolds number at ~80 days after the flow initiation is due to a decrease in the driving pressure gradient that mimics depletion of the magma source (see text for details).

predictions of melt back in channels with developed turbulent flow. Along-strike variations in the dike thickness are proportional to the variations in bulk magma temperature, so they decrease as the channel width (and the thermal entry length) increases. On average, the calculated dike width varies by less than a factor of two (depending on the effective Peclet number) in the flow direction, which is much less than the corresponding variations associated with laminar melt back [*Lister and Dellar*, 1996]. Effects of viscous dissipation on heat transfer during turbulent flow are relatively minor.

7. Discussion

A basic question concerning melt back is how much melt has to pass through a dike in order to widen it to a specified thickness. Figure 10 shows the cumulative amount of magma that "erupted" (flowed out of the channel), per unit height, versus the channel width at the outlet for the range of magma viscosities and different host rock compositions discussed previously. Because our model is two-dimensional, a dike height must be chosen in order to estimate magma volumes. Assuming an effective height of 10 km, one may see that for basaltic magma having viscosity of 50 Pa s [*Shaw*, 1972], an order of magnitude increase in the dike thickness from 10 to 100 m corresponds to 2×10^4 km^3 of discharged magma in the case of granitic crust and almost 10^5 km^3 in the case of basaltic crust (Figure 10b). An increase in thickness from 10 to 50 m requires volumes that are about a factor of 5 less. These volumes may be compared with the estimated volumes of individual lava flows of 10^3-10^4 km^3 [*Shaw and Swanson*, 1970; *Hooper*, 1997], as well as to the total volumes of several millions of cubic kilometers emplaced during the largest flood basalt events [*White and McKenzie*, 1989; *Coffin and Eldholm*, 1994] divided by the associated numbers of feeder dikes of the order of 10^2 [e.g., *Ernst and Buchan*, 1997]. Note that our calculated volumes should be viewed as upper bounds because only a fraction of magma from a dike may make it to the surface and erupt, while the rest may continue propagating laterally. Results shown in Figure 10 illustrate that most of the dike widening occurs when the flow is turbulent. Decreases in magma viscosity (Figure 10a) do not substantially reduce the total volume of magma required to thermally erode a dike conduit (e.g., from 10 to 100 m) because

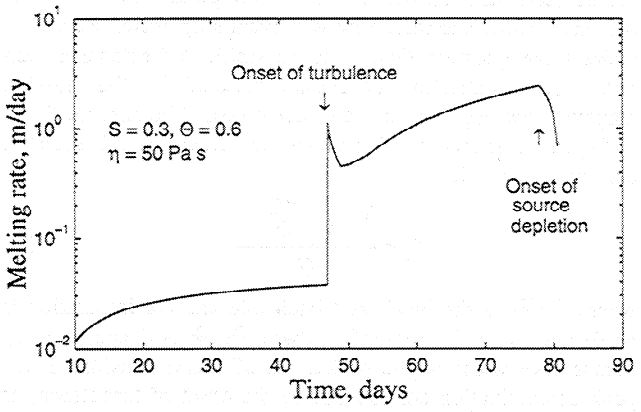

Figure 9. Time evolution of the melt back rate at the channel outlet for the same simulation as shown in Figure 8.

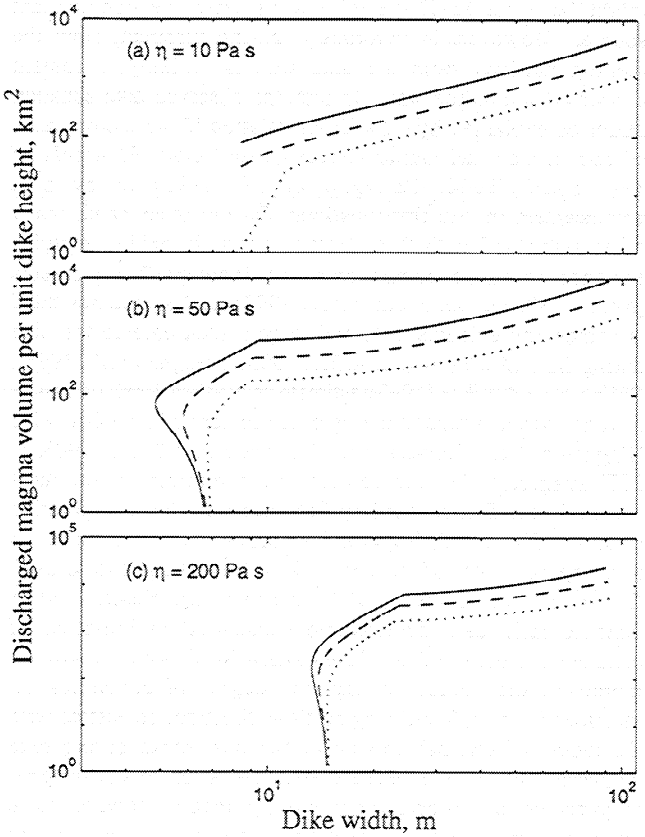

Figure 10. Total amount of magma passed through the dike (i.e., time-integrated flux), per unit dike height, as a function of dike thickness at the outlet, for typical crust compositions and magma viscosities of (a) 10 Pa s, (b) 50 Pa s, and (c) 200 Pa s. Solid curves correspond to basaltic host rocks, dashed curves correspond to andesitic host rocks, and dotted curves represent granitic host rock composition (see Table 1). Initial freezing at the outlet (marked by negative slopes of the curves) is eventually followed by melting; transition from laminar to turbulent melt back is marked by kinks in the curve slopes. For magma viscosity of 10 Pa s the flow is turbulent from the very beginning.

the volume flux is nearly independent of magma viscosity after the onset of turbulence (see equation (23)). On the other hand, elevated magma viscosities increase the total volume of discharged magma required for thermal erosion (Figure 10c); this reflects the retarded onset of turbulence and significant magma volumes passing through the dike during the sustained phase of laminar melt back.

On the basis of the calculations presented above, one may conclude that melt back associated with giant dike emplacement is a viable mechanism and greater efforts may be warranted for its identification in the field. One of the apparent indicators of massive thermal erosion is contamination of the primitive basalt by crustal material. Whether geochemical signatures of flood basalts and associated feeder dikes reflect crustal contamination is still debated; in cases when contamination is inferred, it does not seem to exceed 10-20% [*Mohr*, 1987]. *Gibson et al.* [1987] note that thin dikes in the Mackenzie swarm appear to be chemically homogeneous, while dikes thicker than 30 m are markedly zoned, with the centers being more evolved than the margins. On this basis they concluded that contamination did not occur during (or after) emplacement because the opposite relationship (enriched margins with respect to the center) might be expected if the dike walls were the contaminant source. However, in vigorously mixing turbulent flow the melting material from the dike wall is unlikely to remain concentrated near the wall. In fact, the observed dike zonation might be explained by flow differentiation if the incorporated silica-rich melt had higher viscosity than basalt [*Bhattacharji and Smith*, 1964; *Carrigan et al.*, 1992] or by post emplacement in situ fractionation. On the other hand, many dikes associated with flood basalt events do exhibit margins enriched in felsic components and incompatible elements [*Ross*, 1983; *Philpotts and Asher*, 1993], and sometimes there is compelling evidence that melted wall rock entered the dike during flow [*Philpotts and Asher*, 1993; *Baragar et al.*, 1996]. *Philpotts and Asher* [1993] estimate that at least 6% of crustal material was assimilated during emplacement of the 60-m-wide Higganum dike (Connecticut). *Thirlwall and Jones* [1983, p. 207] suggested that the contamination mechanism for most basalts in the British Tertiary Province was the incorporation of up to 15% of melt from the host rocks which took place "in a complex zone of feeder dykes traversing the crust." *Greenough and Hodych* [1990] note that trace element and Sr isotopic ratio data demonstrate substantial assimilation of continental crust in dikes of the eastern North America swarm; moreover, they point out that the degree of contamination increases in the inferred magma flow direction, consistent with the model of thermal erosion of the host rocks during dike emplacement. This is because assimilation of crustal material is expected to progressively modify magma toward more evolved compositions downstream. The more recent data of *Baragar et al.* [1996] indicate that this may be the case for the Mackenzie dikes. Their Figure 11 shows that crustal contamination (as measured by the K/Ti ratio) is highly variable within ~600 km from the focus of the swarm, but beyond this distance (i.e., where the flow presumably becomes predominantly horizontal), variability decreases and crustal contamination seems to increase. This increase ceases near the downstream termination of the swarm at ~2100 km from the focus. Unfortunately, predictions of our numerical models cannot be directly compared to these observations because *Baragar et al.* [1996] do not systematically report the widths of dikes sampled. Some further examples of crustal contamination, as well as possible alternative explanations, are given by *Mohr* [1987]. In principle, the implication from geochemical data that a crustal isotopic component was introduced to some but not all of the magmas [*Thompson*, 1982] could reflect differences in the amount of assimilation between dikes that erupt and those that do not. For dikes that do not erupt (e.g., if the excess magma pressure is too low or the level of neutral buoyancy is too deep), the driving pressure gradient will decrease with increasing dike length beyond the plume-generated uplift, and at some point the flow may become laminar and melt back will eventually cease. Below we address the question Given the possibility of extensive melt back and assimilation of crustal material by the flowing magma, what degree of contamination should be expected?.

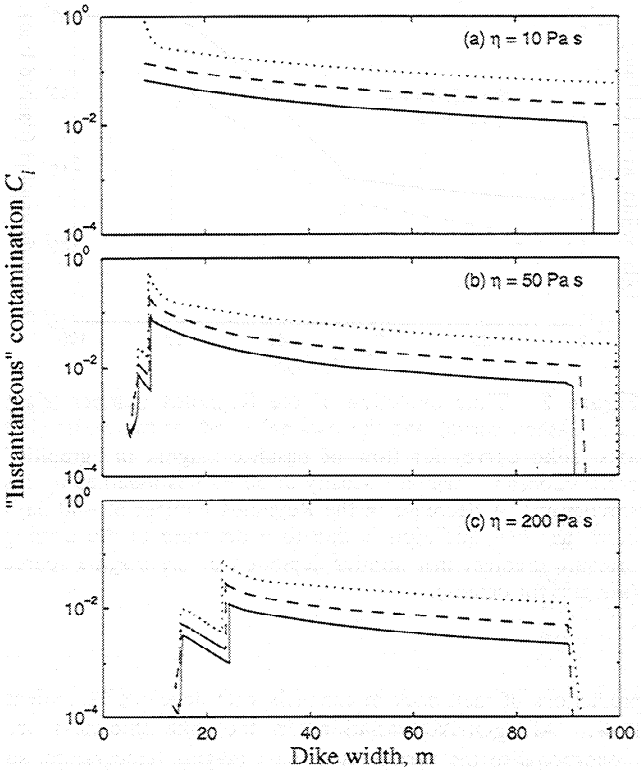

Figure 11. Instantaneous contamination of magma flow in a dike, as defined by (33), for the three host rock compositions given in Table 1 (notation is the same as in Figure 10). Spikes in contamination curves (Figures 11b and 11c) correspond to the onset of laminar and turbulent melt back. In both laminar and turbulent melt back, increases in the assimilation rate are offset by increases in the flow rate, which tends to decrease magma contamination as the dike width increases.

Figure 11 shows the "instantaneous" dike contamination C_i, defined as the ratio

$$C_i = \frac{2\int_{\text{meltback}} \frac{\partial w}{\partial t} dx}{Q}, \qquad (33)$$

where $\partial w/\partial t$ is the local melt back rate and the integration is performed over the region(s) where $\partial w/\partial t > 0$ and $w > w_0$ versus dike width at the outlet. In all cases considered, the peak contamination corresponds to the onset of turbulence; as the Reynolds number (and the dike width) increases beyond the critical value, contamination diminishes. This is because an

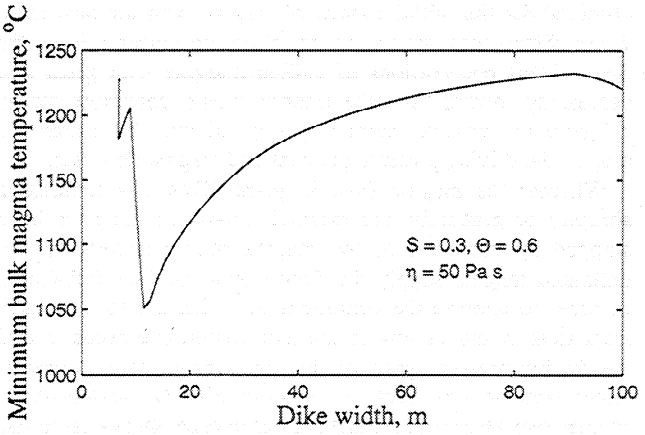

Figure 12. Variations in the minimum bulk magma temperature as a function of the dike width at the outlet for the basalts intruding granitic crust.

increase in the melting (i.e., contamination) rate is offset by an increase in the flow rate and supply of "pure" magma from the source. Similar results were obtained by *Huppert and Sparks* [1985] using steady state calculations. As illustrated by Figure 11, for basaltic crust, contamination is only several percent; for more silicic host rock compositions it may be as high as several tens of percent. While our calculations are likely to overpredict the melting rate and contamination at the onset of turbulence (see Figure 9), it is possible that assimilation of fusible crustal rocks may effectively inhibit a transition to a fully developed turbulent flow by decreasing the bulk magma temperature and increasing the magma viscosity. Figure 12 shows variations in the minimum bulk magma temperature (which is the bulk magma temperature at the channel outlet) versus dike width for granitic host rocks. Shortly after the onset of turbulence the downstream temperature drops by nearly 150°C as a result of massive melting and assimilation. Such a decrease in the bulk magma temperature (plus the dramatic modification of magma composition, see Figure 11) could substantially increase magma viscosity downstream. This could reduce the flow rate and effectively suppress turbulence, so that the overall melt back rate would go down. After the dike width increases beyond 20-30 m the effect of contamination on the overall flow dynamics becomes small (see Figures 11 and 12). Taken at face value, Figure 11 predicts a weak inverse correlation of the bulk SiO_2 content with dike width for dikes wider than a few tens of meters. It is interesting to note that the data shown in Figure 2 qualitatively agree with this prediction (using basalt viscosity as a proxy for SiO_2 content); however, *Wada* [1994] does not report whether the data for giant dikes come from a single swarm. More careful analysis is required to check possible correlations between the dike width and magma composition within different swarms. Figure 13 shows bulk contamination of the erupted magma, C_b, defined as the ratio of the total volume of fused crustal rock to the total volume of magma that flowed out of the channel (essentially, expression (33) with the numerator and denominator integrated over time), as a function of the channel width at the outlet. As one can see from Figure 13, bulk contamination of "flood lavas" in our model varies from <1% (basaltic host rocks) to several percent (granitic host rocks), assuming perfect mixing of the erupted material.

Another problem in understanding the emplacement of giant dike swarms is the origin of chilled margins. As was mentioned above, the presence of chilled margins is often viewed as evidence against thermal erosion and turbulent magma flow in dikes [e.g., *Cadman et al.*, 1990]. However, intrusion of high-solidus-temperature magmas into less refractory host rocks may result in freezing of basalt at the same time that the host rock starts to melt, as predicted theoretically [*Huppert*, 1989; *Huppert and Sparks*, 1989] and inferred from field data [e.g., *Philpotts and Asher*, 1993]. Removal of the basaltic chill (either by remelting or by viscous drag) may give rise to convective mixing of pockets of host rock melt into the bulk of the flow and new contact of basalt with the host. Thus thermal erosion may involve continual formation and removal of basaltic chills at the dike margin. Field observations of chilled contacts with indications of erosion have been reported [*Platten and Watterson*, 1987; *Greenough and Hodych*, 1990]. Upon the termination of flow, chilled margins may or may not be preserved at the magma contacts, so that great spatial variability in the contact structure is to be expected. Sometimes such variability is observed in the field. For example, *Billings* [1925, p. 144] notes that one of the contacts of the Medford dike in eastern Massachusetts (see Figure 1) has a sharp and straight chill, while the other is "wavy, with the appearance of having been corroded." *Ross* [1995] presents strong geochemical evidence of assimilation of felsic country rock during the emplacement of this dike. Similarly, *Bridgewater and Coe* [1970, p. 70] report that one of the Isortoq dikes in south Greenland exhibits chilled

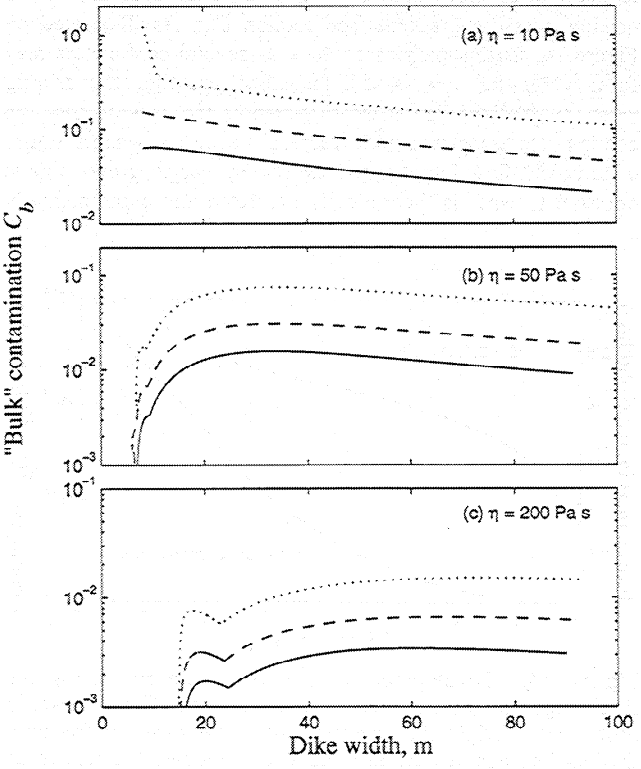

Figure 13. Fraction of the assimilated crustal component in magma that flowed out of the dike (e.g., erupted), as a function of the dike width at the outlet. Notation is the same as in Figures 10 and 11.

margins along one of its contacts and "considerable mixing with melted country rocks" along the other.

Another possible mechanism for forming chilled margins in giant dikes with turbulent flow relates to the dynamics of flow termination. During turbulent melt back, there is a conductive thermal boundary layer in the host rock that travels ahead of the moving phase boundary. Within this layer the temperature falls from the solidus to essentially the far-field temperature. Under steady state conditions the characteristic thickness of this boundary layer is [e.g., *Hulme*, 1975]

$$\delta = \frac{8w}{Nu}\frac{S+\Theta}{\overline{\theta}-\Theta}, \tag{34}$$

where $2w$ is the local dike width and the Nusselt number Nu is given by (31). Dimensionally, δ varies from ~1 m for a 10 m wide dike to ~10 cm for a dike that is 100 m wide (assuming the fluid mechanical and thermophysical parameters used throughout this paper). Because δ is inversely proportional to the melt back rate, flows characterized by stronger turbulence also have larger temperature gradients in the solid near the solid-liquid interface. Therefore, if the flow stops quickly so that the heat transfer in the fluid is dominated by conduction, these large temperature gradients may lead to rapid cooling of the magma and formation of chilled margins at the contact. A necessary condition for such a mechanism is that the timescale of flow termination should not significantly exceed the diffusive timescale for the boundary layer $(\kappa\delta)^{1/2}$. For δ varying from 10 cm to 1 m, the corresponding timescale is of the order of several hours to several days. Figure 14 shows the onset of freezing and variations in the cooling rate at a margin of a 90-m-wide dike in basaltic host rocks ($S = 0.5$, $\Theta = 0.9$). In this case, melt back is reversed, and the frozen margin starts to grow after more than 2 days of a linear decrease in the driving pressure gradient (see section 6). As illustrated by Figure 14, frozen margins as thick as several centimeters may form while the flow is still turbulent, provided the driving pressure gradient decreases sufficiently fast. Note that the cooling rate associated with freezing during the waning stages of turbulent flow increases as the frozen margin grows; this is opposite to what is theoretically predicted and experimentally observed for the initial contact of magma with the host rock. These differences should, in principle, be discernible in the field. Thus observations of chilled margins with grain size decreasing toward the dike interior would constitute strong evidence for massive thermal erosion followed by a dramatic drop in the driving pressure gradient and magma flow rate.

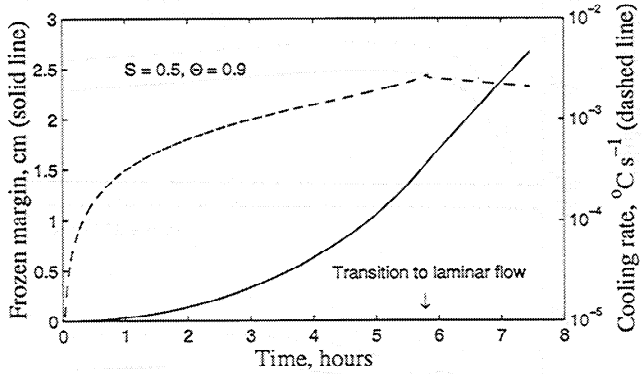

Figure 14. Development of the frozen margin during the final stages of magma flow in a 90-m-wide dike in basaltic host rocks. Origin time corresponds to the onset of freezing. Dashed line denotes the associated cooling rate (calculated as the product of the margin growth rate and the temperature gradient in the solid at the solid-liquid interface). Arrow marks a transition to laminar flow ~5.8 hours after the onset of freezing.

Whether the magma flow in giant dikes was terminated abruptly or gradually, the thermal runaway must have been stopped by depletion of the magma source (otherwise, for unlimited magma supply the flow would continue infinitely). In order to analyze the conditions at which the solidification front steadily moves toward the dike center, one needs to find the driving pressure gradient that corresponds to the onset of either laminar melt back G_l or turbulence G_t, whichever is smaller (we assume that sustained turbulence always gives rise to melt back). For laminar flows in which advection of heat from the source is large compared to viscous dissipation (see section 5), G_l is given by [*Lister and Dellar*, 1996]

$$G_l = Pe_c\frac{\kappa\eta H}{w^4}, \tag{35}$$

where $Pe_c \sim O(10^2)$ is the critical Peclet number corresponding to the onset of laminar melt back, and w should be interpreted as an average dike half width. From (2)-(3) the driving pressure gradient corresponding to the onset of turbulence is

$$G_t = Re_c\frac{\eta^2}{w^3\rho_m}, \tag{36}$$

where $Re_c \sim O(10^3)$ is the critical Reynolds number. By comparing (35) and (36) we infer that as the driving pressure gradient decreases, dikes that are thicker than several tens of meters make a transition to laminar flow when G_l is large enough to induce laminar melt back (given the parameters used throughout this paper). Even though one could get initial development of a chilled margin by one of the mechanisms discussed above, preservation of such a chilled margin would require decreases in the driving pressure gradient at a rate that would prevent the onset of laminar melt back.

Using the definition of G_l in (35), one can see that critical driving pressure gradients corresponding to the onset of "steady" freezing in the laminar regime range from a few pascals per meter for dikes that are a few tens of meters thick to $<10^{-3}$ Pa/m for dikes that are ~10^2 m thick. Given that the critical driving pressure gradient strongly decays with increasing w ($G_l \propto w^{-4}$ and $G_t \propto w^{-3}$), shear stresses generated at the dike wall upon the cessation of melt back ($\sim wG$) also decrease with increasing dike thickness. This suggests that wider dikes may have less tendency to produce consistent alignment of the flow fabric. Although initial frozen margins might form at shear stresses that are fairly high (e.g., while the flow is still turbulent), these margins are unlikely to be more than several centimeters thick (see Figure 14 and discussion above), and thus they are not typically sampled in the field studies of the magma flow indicators [e.g., *Ernst and Baragar*, 1992]. Less systematic fabric alignment should also be expected if thermal or compositional convection develops in a dike after the termination of flow. This may explain why, in some cases, measurements of the anisotropy of magnetic susceptibility strongly indicate a horizontal flow direction (e.g., for the Mackenzie dikes [*Ernst and Baragar*, 1992]), while in other cases the patterns of magma flow are much less consistent [e.g., *Ernst and Duncan*, 1995]. In any case, it

should be emphasized that given the probability of extensive melt back during giant dike intrusion, measurements of magnetic fabric most likely record late (and not initial) magma flow directions.

Note that the small "terminal" driving pressure gradient required to permit freezing implies large underpressures in the source magma chamber in order to compensate for the driving pressure gradient due to topography. If a dike erupts at the perimeter of a topographic swell 2 km high, this gives rise to underpressures of the order of 50 MPa. Given such underpressures, it is even possible that collapse of the shallow magma plumbing system may accompany the cessation of flow in giant dikes. On Venus, collapse structures are commonly associated with novae and coronae [*Head et al.*, 1992; *Ernst et al.*, 1995]. Pressure reductions that accompany the arrest of flow may, in principle, reverse the magma flow direction within a dike (e.g., cause the magma to retreat toward the LNB as the dike height decreases). *Philpotts and Asher* [1994] report evidence for a complex history of magma motion during the last stages of giant dike emplacement, based on a careful analysis of magma flow indicators. This may reflect either a flow reversal due to a reduction in source pressure or convection effects mentioned above. The possibility of large "upstream" underpressures also suggests that the dike widths observed in the field may be substantially less than the corresponding dike widths at the time of magma emplacement (for magma underpressures of several tens of megapascals, the elastic decreases in dike width are of the order of several tens of meters, see equation (4)). If so, the stress state that is "frozen in" upon dike solidification is likely to be more extensional than that prior to dike emplacement. Such "self-induced" extension is likely to affect subsequent dike intrusions by introducing large vertical and horizontal gradients in the dike-perpendicular stress (see section 2). This may alleviate the problem of space for the emplacement of giant radiating dike swarms [*Baragar et al.*, 1996].

8. Conclusions

We considered fluid mechanical and thermodynamic aspects of magma emplacement in giant dike swarms by simulating laminar and turbulent flows of hot viscous fluid in semi-infinite and finite channels. For a conduit that is unbounded in the flow direction (e.g., a laterally propagating dike), there exists a critical Brinkman number separating dikes that eventually freeze from those that produce melt back for as long as the magma supply lasts. For conditions appropriate for dike emplacement in plume-related swarms, dike thicknesses of <10 m are sufficient to generate the critical Brinkman numbers. This is an order of magnitude less than observed thicknesses. An order of magnitude increase in dike thickness may have resulted from thermal erosion of the ambient rocks during turbulent magma flow by magma volumes that are in reasonable agreement with the estimated volumes of lava flows in continental flood basalts. Overall magma contamination resulting from assimilation of crustal material is predicted to be <10%, which does not contradict available geochemical data. The chilled margins associated with many giant dikes do not constitute strong evidence against turbulent melt back and massive assimilation of crustal material. They may form during thermal erosion if the host rock melting temperature is less than the solidus of the intruding magma or at the final stage of dike propagation if turbulent flow is quickly terminated. For these reasons, measurements of magnetic fabric most likely reflect the late stages of magma emplacement. For dikes propagating off long-wavelength topographic uplifts (e.g., due to mantle plume heads) and erupting at the uplift periphery, massive thermal erosion implies large magma underpressures and increased extensional stresses in the central part of the uplift. These extensional stresses may provide important controls on the geometry and dynamics of the dike swarm emplacement.

Appendix

In section 6 we wished to obtain equation governing the along-dike variations in the bulk magma temperature $\overline{T}$ (see equation (21)). In order to do so, one may integrate energy conservation equation (5) over the channel half width (we assume symmetry about the channel centerline $y = 0$; see Figure 3),

$$\int_0^{w(x,t)} \frac{\partial T}{\partial t} dy = \kappa \int_0^{w(x,t)} \frac{\partial^2 T}{\partial y^2} dy - \int_0^{w(x,t)} u_x \frac{\partial T}{\partial x} dy - \int_0^{w(x,t)} u_y \frac{\partial T}{\partial y} dy + \frac{\eta}{\rho_m c} \int_0^{w(x,t)} D dy. \quad \text{(A1)}$$

Conductive heat loss term (first term on the right-hand side) in (A1) can be immediately evaluated to yield $\kappa \partial T/\partial y|_{y=-w}$ (given zero heat flux across the channel centerline). Provided that most of the (nonfluctuating) temperature variations across the channel are concentrated in a thin boundary layer near the channel wall (i.e., if $T(y) = \tilde{T} = \text{const}$ for $0 < y < w-\delta$, where $\delta << w$ is the boundary layer thickness), the along-stream advection term (second term on the right-hand side of (A1)) gives rise to

$$\int_0^{w(x,t)} u_x \frac{\partial T}{\partial x} dy = \int_0^{w(x,t)-\delta} u_x \frac{\partial T}{\partial x} dy + \int_{w(x,t)-\delta}^{w(x,t)} u_x \frac{\partial T}{\partial x} dy = \frac{\partial \tilde{T}}{\partial x} \int_0^{w(x,t)-\delta} u_x dy + O\left(\delta u_x(\delta) \frac{\partial \tilde{T}}{\partial x}\right). \quad \text{(A2)}$$

The integral over the boundary layer (second addend on the right-hand side) in (A2) is of the order of δ and thus may be omitted. Similarly, one can show that the across-stream advection (third term on the right-hand side of (A1)) is $O(\delta u_y(\delta) \partial T/\partial y|_{y=-w}$. Because the latter may be significant compared to molecular diffusion (see the first term on the right-hand side in (A1)), we introduce effective thermal diffusivity $\kappa_e \sim \kappa + \int_0^{\delta} u_y dy$ and lump across-stream conduction and across-stream advection in one term that is proportional to the temperature gradient at the dike wall, $\kappa_e \partial T/\partial y|_{y=-w}$. Upon proper nondimensionalization the effective thermal diffusivity κ_e essentially becomes the Nusselt number Nu that quantifies heat losses in a turbulent boundary layer (see (27) and (30)-(31)). The following relationships also hold provided $\delta << w$:

$$\int_0^{w(x,t)-\delta} u_x dy \approx \int_0^{w(x,t)} u_x dy = \frac{Q}{2}, \quad \text{(A3)}$$

where Q is a 2-D volume flux, and

$$\overline{T} \approx \tilde{T}, \quad \text{(A4)}$$

where $\overline{T}$ is the bulk flow temperature defined by (21), and $\tilde{T}$ is the temperature of the isothermal core of the flow. Dividing

(A1) by the channel half width w and making use of (A2)-(A4), we obtain

$$\frac{1}{w}\int_0^w \frac{\partial T}{\partial t}dy = \frac{\kappa_e}{w}\left.\frac{\partial T}{\partial y}\right|_{y=w} - \frac{Q}{2w}\frac{\partial \overline{T}}{\partial x} + \frac{\eta}{\rho_m c w}\int_0^w D dy. \qquad \text{(A5)}$$

We estimate viscous dissipation term (last term on the right-hand side in (A5)) using the total amount of work spent on viscous pressure losses in the fluid; this work is given (up to a dimensional constant) by a product of the cross-sectionally averaged fluid velocity and local driving pressure gradient $\partial p/\partial x$, i.e.,

$$\frac{\eta}{\rho_m c w}\int_0^w D dy \approx \frac{Q}{2\rho_m c w}\frac{\partial p}{\partial x}. \qquad \text{(A6)}$$

Substituting (A6) into (A5) and noting that

$$\frac{\partial}{\partial t}\left(\frac{1}{w}\int_0^w T dy\right) = -\frac{1}{w^2}\frac{\partial w}{\partial t}\int_0^w T dy + \frac{1}{w}\left[\frac{\partial w}{\partial t}T(w) + \int_0^w \frac{\partial T}{\partial t}dy\right] =$$

$$\frac{1}{w}\int_0^w \frac{\partial T}{\partial t}dy - \frac{1}{w}\frac{\partial w}{\partial t}\left(\overline{T} - T_s\right), \qquad \text{(A7)}$$

where $T(w) = T_s$ is the channel wall (i.e., magma freezing) temperature, one may obtain (22).

Acknowledgments. We thank Steve Emerman and Frank Spera for thorough reviews that improved the quality of this manuscript. This work was supported by NSF grant OCE-9617696.

References

Anderson, D.L., The edges of the mantle, in *The Core-Mantle Boundary Region, Geodyn. Ser.*, vol. 28, edited by M. Gurnis et al., pp. 255-271, AGU, Washington, D. C., 1998.

Baragar, W.R.A., R.E. Ernst, L. Hulbert, and T. Peterson, Longtitudinal petrochemical variations in the Mackenzie dyke swarm, northwestern Canadian shield, *J. Petrol., 37*, 317-359, 1996.

Barsukov, V.L. et al., The geology and geomorphology of the Venus surface as revealed by radar images obtained by Venera 15 and 16, *J. Geophys. Res., 91*, 378-398, 1986.

Batchelor, G.K., *An Introduction to Fluid Dynamics*, 615 pp., Cambridge Univ. Press, New York, 1967.

Bhattacharji, S., and C.H. Smith, Flowage differentiation, *Science, 145*, 150-153, 1964.

Billings, M.P., On the mechanics of dike intrusion, *J. Geol., 33*, 141-150, 1925.

Bird, R.B., W.E. Stewart, and E.N. Lightfoot, *Transport Phenomena*, John Wiley, New York, 1970.

Bridgewater, D., and K. Coe, The role of stoping in the emplacement of the giant dikes of Isortoq, South Greenland, in *Mechanism of Igneous Intrusion*, edited by G. Newall, pp. 67-78, Gallery, Liverpool, England, 1970.

Bruce, P.M., and H.E. Huppert, Solidification and melting along dikes by the laminar flow of basaltic magma, in *Magma Transport and Storage*, edited by M.P. Ryan, pp. 87-101, John Wiley, New York, 1990.

Cadman, A., J. Tarney, and R.G. Park, Intrusion and crystallization features in Proterozoic dyke swarms, in *Mafic Dykes and Emplacement Mechanisms*, edited by A.J. Parker, P.C. Rickwood, and D.H. Tucker, pp. 13-24, A.A. Balkema, Brookfield, Vt., 1990.

Carrigan, C.R., G. Schubert, and J.C. Eichelberger, Thermal and dynamical regimes of single- and two-phase magmatic flow in dikes, *J. Geophys. Res., 97*, 17,377-17,392, 1992.

Coffin, M.F., and O. Eldholm, Large igneous provinces: Crustal structure, dimensions, and external consequences, *Rev. Geophys., 32*, 1-36, 1994.

Courtillot, V.E., Mass extinctions in the last 300 million years: one impact and seven flood basalts, *Isr. J. Earth Sci., 43*, 259-266, 1994.

Cox, K.G., The role of mantle plumes in the development of continental drainage patterns, *Nature, 342*, 873-876, 1989.

Dean, R.B., Reynolds number dependence of skin friction and other bulk flow variables in two-dimensional rectangular duct flow, *ASME J. Fluids Eng., Ser. D, 100*, 215, 1978.

Delaney, P.T., and D.D. Pollard, Solidification of basaltic magma during flow in dike, *Am. J. Sci., 282*, 856-885, 1982.

Duncan, R.A., and M.A. Richards, Hotspots, mantle plumes, flood basalts, and true polar wander, *Rev. Geophys, 29*, 31-50, 1991.

Einarsson, P., and B. Brandsdottir, Seismological evidence for lateral magma intrusion during the July 1978 deflation of the Krafla volcano in NE-Iceland, *J. Geophys., 47*, 160-165, 1980.

Ernst, R.E., and W.R.A. Baragar, Evidence from magnetic fabric for the flow pattern of magma in the Mackenzie giant radiating dyke swarm, *Nature, 356*, 511-513, 1992.

Ernst, R.E., and K.L. Buchan, Giant radiating dyke swarms: Their use in identifying Pre-Mesozoic large igneous provinces and mantle plumes, in *Large Igneous Provinces: Continental, Oceanic and Planetary Flood Volcanism, Geophys. Monogr. Ser.*, vol. 100, edited by J.J. Mahoney and M.F. Coffin, pp. 297-334, AGU, Washington, D. C., 1997.

Ernst, R.E., and A.R. Duncan, Magma flow in the giant Botswana dyke swarm from analysis of magnetic fabric, in *Program and abstracts of 3rd International Dyke Conference*, edited by A. Agnon and G. Baer, p. 30, Jerusalem, Israel, 1995.

Ernst, R.E., J.W. Head, E. Parfitt, E. Grosfils, and L. Wilson, Giant radiating dike swarms on Earth and Venus, *Earth Sci. Rev., 39*, 1-58, 1995.

Fahrig, W.F., The tectonic setting of continental mafic dyke swarms: Failed arm and early passive margin, in *Mafic Dyke Swarms*, edited by H.C. Halls and W.F. Fahrig, *Geol. Assoc. Can. Spec. Pap., 34*, 331-348, 1987.

Fedotov, S.A., Ascent of basic magmas in the crust and the mechanism of basaltic fissure eruptions, *Int. Geol. Rev., 20*, 33-48, 1978.

Fialko, Y.A., and A.M. Rubin, Thermodynamics of lateral dike propagation: Implications for crustal accretion at slow spreading mid-ocean ridges, *J. Geophys. Res., 103*, 2501-2514, 1998.

Fialko, Y.A., and A.M. Rubin, What controls the along-strike slopes of volcanic rift zones?, *J. Geophys. Res.*, in press, 1999.

Fox, C.G., W.E. Radford, R.P. Dziak, T.-K. Lau, H. Matsumoto, and A.E. Schreiner, Acoustic detection of a seafloor spreading episode on the Juan de Fuca Ridge using military hydrophone arrays, *Geophys. Res. Lett., 22*, 131-134, 1995.

Fujii, N., and S. Uyeda, Thermal instabilities during flow of magma in volcanic conduits, *J. Geophys. Res., 79*, 3367-3369, 1974.

Gibson, I.L., M.N. Sinha, and W.F. Fahrig, The geochemistry of the Mackenzie dyke swarm, Canada, in *Mafic Dyke Swarms*, edited by H.C. Halls and W.F. Fahrig, *Geol. Assoc. Can. Spec. Pap., 34*, 109-121, 1987.

Gill, R.C.O., A.K. Pedersen, and J.G. Larsen, Tertiary picrites in West Greenland: Melting at the periphery of a plume?, in *Magmatism and the Causes of Continental Break-up*, edited by B.C. Storey, T. Alabaster, and R.J. Pankhurst, *Geol. Soc. Spec. Publ., London, 68*, 335-348, 1992.

Gnielinski, V., New equations for heat and mass transfer in turbulent pipe and channel flow, *Int. Chem. Eng., 16*, 359-368, 1976.

Greenough, J.D., and J.P. Hodych, Evidence for lateral magma injection in the early Mesozoic dykes of eastern North America, in *Mafic Dykes and Emplacement Mechanisms*, edited by A.J. Parker, P.C. Rickwood, and D.H. Tucker, pp. 35-46, A.A. Balkema, Brookfield, Vt., 1990.

Griffiths, R.W., and I.H. Campbell, Stirring and structure in mantle starting plumes, *Earth Planet. Sci. Lett.*, 99, 66-78, 1990.

Grosfils, E.B., and J.W. Head, The global distribution of giant radiating dike swarms on Venus: Implications for the global stress state, *Geophys. Res. Lett., 21*, 701-704, 1994.

Halls, H.C., and W.F. Fahrig (Eds.) Mafic Dyke Swarms, *Geol. Assoc. Can. Spec. Pap., 34*, 503 pp., 1987.

Hardee, H.C., and D.W. Larson, Viscous dissipation effects in magma conduits, *J. Volcanol. Geotherm. Res., 2*, 229-308, 1977.

Head, J.W., L.S. Crumpler, J.C. Aubele, J.E. Guest, and R.S. Saunders, Venus volcanism: Classification of volcanic features and structures, associations and global distribution from Magellan data, *J. Geophys. Res., 97*, 13,153-13,197, 1992.

Hickman, S.H., Stress in the lithosphere and the strength of active faults, *U.S. Natl. Rep. Int. Union Geol. Geophys., 1987-1990, Rev. Geophys., 29*, 759-775, 1991.

Hill, R.I., I.H. Campbell, G.F. Davies, and R.W. Griffith, Mantle plumes and continental tectonics, *Science, 256*, 186-193, 1992.

Hirs, G.G., A systematic study of turbulent film flow, *J. Lubric. Technol., 96*, 118-126, 1974.

Holman, J.P., *Heat Transfer*, 8th ed., 696 pp., McGraw-Hill, New York, 1997.

Hooper, P.R., The timing of crustal extension and the eruption of continental flood basalts, *Nature, 345*, 246-249, 1990.

Hooper, P.R., The Columbia river flood basalt province: Current status, in *Large Igneous Provinces: Continental, Oceanic and Planetary Flood Volcanism, Geophys. Monogr. Ser.*, vol. 100, edited by J.J. Mahoney and M.F. Coffin, pp. 1-28, AGU, Washington, D. C., 1997.

Hulme, G., Turbulent lava flow and the formation of lunar sinuous rilles, *Mod. Geol., 4*, 107-117, 1975.

Huppert, H.E., Phase changes following the initiation of a hot turbulent flow over a cold solid surface, *J. Fluid Mech., 198*, 293-319, 1989.

Huppert, H.E., and R.S.J. Sparks, Cooling and contamination of mafic and ultramafic magmas during ascent through continental crust, *Earth Planet. Sci. Lett., 74*, 371-386, 1985.

Huppert, H.E., and R.S.J. Sparks, Chilled margins in igneous rocks, *Earth Planet. Sci. Lett., 92*, 397-405, 1989.

Kays, W.M., and M.E. Crawford, *Convective Heat and Mass Transfer*, 601 pp., McGraw-Hill, New York, 1993.

Kerr, R.C., and J.R. Lister, Comment on "On the relationship between dike width and magma viscosity" by Yutaka Wada, *J. Geophys. Res., 100*, 15,541, 1995.

Khazan, Y.M., and Y.A. Fialko, Fracture criteria at the tip of fluid-driven cracks in the Earth, *Geophys. Res. Lett., 22*, 2541-2544, 1995.

Klein, F., R.Y. Koyanagi, J.S. Nakata, and W.R. Tanigawa, The seismicity of Kilauea's magma system, in *Volcanism in Hawaii*, edited by R.W. Decker, T.L. Wright, and P.H. Stauffer, *U.S. Geol. Surv. Prof. Pap., 1350*, 1019-1186, 1987.

Kretz, R., R. Hartee, D. Garret, and C. Cermignani, Petrology of the Grenville swarm of gabbro dikes, Canadian precambrian shield, *Can. J. Earth Sci., 22*, 53-71, 1985.

Kutateladze, S.S., *Fundamentals of Heat Transfer*, 485 pp., Academic, San Diego, Calif., 1963.

Landau, L.D., and E.M. Lifshitz, *Theory of Elasticity*, 187 pp., Pergamon, Tarrytown, N.Y., 1986.

Lassiter, J.C., and D.J. DePaolo, Plume/lithosphere interaction in the generation of continental and oceanic flood basalts: Chemical and isotopic constraints, in *Large Igneous Provinces: Continental, Oceanic and Planetary Flood Volcanism, Geophys. Monogr. Ser.*, vol. 100, edited by J.J. Mahoney and M.F. Coffin, pp. 335-356, AGU, Washington, D. C., 1997.

LeCheminant, A.N., and L.M. Heaman, Mackenzie igneous events, Canada: Middle Proterozoic hotspot magmatism associated with ocean opening, *Earth Planet. Sci. Lett., 96*, 38-48, 1989.

Lister, J.R., Buoyancy-driven fluid fracture: Similarity solutions for the horizontal and vertical propagation of fluid-filled cracks, *J. Fluid Mech., 217*, 213-239, 1990.

Lister, J.R., and P.J. Dellar, Solidification of pressure-driven flow in a finite rigid channel with application to volcanic eruptions, *J. Fluid Mech., 323*, 267-283, 1996.

Lister, J.R., and R.C. Kerr, Fluid-mechanical models of crack propagation and their application to magma transport in dykes, *J. Geophys. Res., 96*, 10,049-10,077, 1991.

McConnel, R.K., Dike propagation, in *Economic Geology in Massachusetts*, edited by O.C. Farquhar, pp. 97-104, Univ. Mass. Grad. Sch., Amherst, 1967.

McKenzie, D., and F. Nimmo, The generation of martian floods by the melting of ground ice above dykes, *Nature, 397*, 231-233, 1999.

McKenzie, D., J.M. McKenzie, and R.S. Saunders, Dike emplacement on Venus and on Earth, *J. Geophys. Res., 97*, 15,977-15,990, 1992.

Mohr, P.A., Crustal contamination in mafic sheets: A summary, in *Mafic Dyke Swarms*, edited by and H.C. Halls and W.F. Fahrig, *Geol. Assoc. Can. Spec. Pap., 34*, 75-80, 1987.

Morgan, W.J., Convection plumes in the lower mantle, *Nature, 230*, 42-43, 1971.

Morgan, W.J., Hotspot tracks and the early rifting of the Atlantic, *Tectonophysics, 94*, 123-139, 1983.

Parfitt, E.A., and J.W. Head, Buffered and unbuffered dike emplacement on Earth and Venus: Implications for magma reservoir size, depth, and rate of magma replenishment, *Earth Moon Planets, 61*, 249-261, 1993.

Parker, A.J., P.C. Rickwood, and D.H. Tucker (Eds.) *Mafic Dykes and Emplacement mechanisms*, 541 pp., A.A. Balkema, Brookfield, Vt., 1990.

Petukhov, B.S., and A.F. Polyakov, *Heat Transfer in Turbulent Mixed Convection*, 216 pp., Hemisphere, New York, 1988.

Philpotts, A.R., and P.M. Asher, Wallrock melting and reaction effects along the Higganum diabase dike in Connecticut: Contamination of a continental flood basalt feeder, *J. Petrol., 34*, 1029-1058, 1993.

Philpotts, A.R., and P.M. Asher, Magmatic flow-direction indicators in a giant diabase feeder dike, Connecticut, *Geology, 22*, 363-366, 1994.

Platten, I.M., and J. Watterson, Magma flow and crystallization in dyke fissures, in *Mafic Dyke Swarms*, edited by and H.C. Halls and W.F. Fahrig, *Geol. Assoc. Can. Spec. Pap., 34*, 65-73, 1987.

Pollard, D.D., Elementary fracture mechanics applied to the structural interpretation of dykes, in *Mafic Dyke Swarms*, edited by and H.C. Halls and W.F. Fahrig, *Geol. Assoc. Can. Spec. Pap., 34*, 5-24, 1987.

Richardson, W.A., The problem of batholitic intrusion, *Geol. Mag., 60*, 121-131, 1923.

Ross, M.E., Chemical and mineralogic variations within four dikes of the Columbia River Basalt Group, southeastern Columbia Plateau, *Geol. Soc. Am. Bull., 94*, 1117-1126, 1983.

Ross, M.E., Crustal contamination of mafic dyke magmas, in in *Program and abstracts of 3rd International Dyke Conference*, edited by A. Agnon and G. Baer, p. 58, Jerusalem, Israel, 1995.

Shaw, H.R., Viscosities of magmatic silicate liquids: An empirical method of prediction, *Am. J. Sci., 272*, 870-893, 1972.

Shaw, H.R., and D.A. Swanson, Eruption and flow rates of flood basalts, in *Proc. Second Columbia River Basalt Symposium*, edited by E.H. Gilmour and D. Stradling, pp. 271-299, Eastern Washington State College Press, Cheney, 1970.

Sigurdsson, H., Dyke injection in Iceland: A review, in *Mafic Dyke Swarms*, edited by H.C. Halls and W.H. Fahrig, *Geol. Assoc. Can. Spec. Pap., 34*, 55-64, 1987.

Spence, D. A., and D. L. Turcotte, Magma-driven propagation of cracks, *J. Geophys. Res., 90*, 575-580, 1985.

Stofan, E.R., V.L. Sharpton, G. Schubert, G. Baer, D.L. Bindschadler, D.M. Janes, and S.W. Squyres, Global distribution and characteristics of coronae and related features on Venus: Implications for origin and relation to mantle processes, *J. Geophys. Res., 97*, 13,347-13,378, 1992.

Stothers, R.B., Flood basalts and extinction events, *Geophys. Res. Lett., 20*, 1399-1402, 1993.

Thirlwall, F., and N.W. Jones, Isotope geochemistry and contamination mechanics of Tertiary lavas from Skye, Northwest Scotland, in *Continental Basalts and Mantle Xenoliths*, edited by C.J. Hawkesworth and M.J. Norry, pp. 186-208, Shiva, Cambridge, Mass., 1983.

Thompson, R.N., Magmatism of the British Tertiary Volcanic Province, *Scott. J. Geol., 18*, 49-107, 1982.

Upton, B.G.J., The alkaline province of south-west Greenland, in *The Alkaline Rocks*, edited by H. Sorensen, pp. 221-237, John Wiley, New York, 1974.

Wada, Y., On the relationship between dike width and magma viscosity, *J. Geophys. Res., 99*, 17,743-17,755, 1994.

Walker, G.P.L., P.R. Eyre, S.R. Spengler, M.D. Knight, and K. Kennedy, Congruent dike widths in large basaltic volcanoes, in *Physics and Chemistry of Dykes*, edited by G. Baer and A. Heimann, pp. 41-49, A.A. Balkema, Brookfield, Vt., 1995.

Watson, S., and D. McKenzie, Melt generation by plumes: A study of Hawaiian volcanism, *J. Petrol., 32*, 501-537, 1991.

White, R.S., and D. McKenzie, Magmatism at rift zones: The generation of volcanic continental margins and flood basalts, *J. Geophys. Res., 94*, 7685-7729, 1989.

Y.A. Fialko, Seismo Lab 252-21, California Institute of Technology, Pasadena, CA 91125. (email: fialko@gps.caltech.edu)

A.M. Rubin, Department of Geosciences, Princeton University, Princeton, NJ 08544. (e-mail: allan@geo.princeton.edu).

(Received September 28, 1998; revised May 12, 1999; accepted June 11, 1999.)